M. Ishihara : *Nucl. Phys. A*, **588**, 241c (1995).
5) S. Motomura, Y. Yang, Y. Gono, S. Enomoto, Y. Yano, K. Asahi : *RIKEN Review*, **35**, 116 (2001).
6) S. Motomura, S. Enomoto, H. Haba, K. Igarashi, Y. Gono, Y. Yano : *IEEE Transact Nucl. Sci.*, **54**(3), 710 (2007).
7) V. Schönfelder, A. Hirner, K. Schneider : *Nucl. Instr. Methods*, **107**, 385 (1973).
8) R. W. Todd, J. M. Nightingale, D. B. Everett : *Nature*, **251**, 132 (1974).
9) S. Motomura, Y. Kanayama, H. Haba, Y. Watanabe, S. Enomoto : *J. Anal. At. Spectrom.*, **23**, 1089 (2008).
10) A. Takeda, H. Tamano, S. Enomoto, N. Oku, : *Cancer Res.*, **61**, 5065 (2001).
11) H. Tamano, R. Hirunuma, S. Enomoto, A. Takeda : *RIKEN Review*, **35**, 57 (2001).
12) M. A. Deleplanque, I. Y. Lee, K. Vetter, G. J. Schmid, F. S. Stephens, R. M. Clark, R. M. Diamond, P. Fallon, A. O. Macchiavelli : *Nucl. Instr. Meth. A*, **430**, 292 (1999).
13) R. C. Rohe, M. M. Sharfi, K. A. Kecevar, J. D. Valentine, C. Bonnerave : *IEEE Trans Nucl. Sci.*, **44**(6), 2477 (1997).
14) S. Watanabe, S. Takeda, S. N. Ishikawa, H. Odaka, M. Ushio, T. Tanaka, K. Nakazawa, T. Takahashi, H. Tajima, Y. Fukazawa, Y. Kuroda, M. Onishi : *Nucl. Instr. Meth. A*, **579**, 871 (2007).
15) S. Kabuki, K. Hattori, R. Kohara, E. Kunieda, A. Kubo, H. Kubo, K. Miuchi, T. Nakahara, T. Nagayoshi, H. Nishimura, Y. Okada, R. Orito, H. Sekiya, T. Shirahata, A. Takeda, T. Tanimori, K. Ueno : *Nucl. Instr. Meth. A*, **580**, 1031 (2007).

Three-Dimensional Tomographic Imaging by Semiconductor Compton Camera GREI for Multiple Molecular Simultaneous Imaging

Shinji Motomura, Tomonori Fukuchi, Yousuke Kanayama, Hiromitsu Haba, Yasuyoshi Watanabe, and Shuichi Enomoto

***Abstract*–We have investigated the possibility of three-dimensional (3D) tomographic imaging by semiconductor Compton cameras that we have been developing for multiple molecular simultaneous imaging. As a significant feature of Compton cameras, multi-directional projection of the γ-ray source distribution can be obtained even by a fixed-angle imaging with a single Compton camera unit. We have already implemented a 3D tomographic image reconstruction method applicable for both single- and multiple-unit Compton cameras, and succeeded in 3D tomographic imaging with a single Compton camera unit. In order to enlarge the field of view and to obtain more accurate images, we are constructing an array of multiple semiconductor Compton camera units.**

I. Introduction

Recent progress in life science research seems to be beginning to cause a demand for simultaneous imaging analysis of multiple molecular targets in medical diagnosis. Innovations in DNA analysis technology enabled genome-wide association study (GWAS), which revealed that various common diseases, including cancer and metabolic diseases, are multifactorial diseases that are related to genetic polymorphism. Integrated omics in system biology would unveil the molecular pathogenic mechanism of the common diseases.

If we can apply multiple molecular simultaneous imaging (MMSI) for these results, exceedingly accurate and early diagnosis would be realized. GREI [1,2], which is a semiconductor Compton camera, is a promising γ-ray imager being developed for MMSI. It is composed of two double-sided orthogonal-strip germanium detectors arranged in parallel, and the excellent energy resolution and wide energy range allow simultaneous imaging of different molecular probes labeled with different radionuclides. Furthermore, since Compton cameras need no mechanical collimators, there is no loss of γ rays caused by the collimation, and multidirectional projection of the γ-ray source distribution can be obtained even by a fixed-angle imaging with a single Compton camera. Thus, multiple molecular imaging is a natural application of GREI. Among our R&D activities, this paper focuses on three-dimensional tomographic imaging by GREI.

S. Motomura, T. Fukuchi, Y. Kanayama, H. Haba, and S. Enomoto are with Metallomics Imaging Research Unit, RIKEN Center for Molecular Imaging, 6-7-3 Minatojima-minamimachi, Chuo-ku, Kobe 650-0047, Japan (e-mail: motomura@riken.jp).

Y. Watanabe is with Molecular Probe Dynamics Laboratory, RIKEN Center for Molecular Imaging, 6-7-3 Minatojima-minamimachi, Chuo-ku, Kobe 650-0047, Japan.

II. 3D Tomographic Imaging by GREI

In order to obtain accurate 3D distribution of molecular probes in an intact animal or human body, we need to construct tomographic images for each molecular probe. We have already implemented a 3D tomographic image reconstruction method applicable for both single- and multiple-head Compton cameras that is based on the simple backprojection-deconvolution scheme. With this scheme, the 3D tomographic image reconstruction comes down to the problem of deconvolution of point-spread function (PSF).

In order to obtain accurate 3D tomographic images with this method, we have implemented 3D PSF that is dependent on the γ-ray source position. The problem was that the naive implementation of the PSF results in a huge size matrix that is hard to implement. Thus we have conceived a dynamic PSF generation method, in which the PSF for each source position is calculated by interpolation of the small number of predefined PSFs (Fig. 1). This method allows us to obtain accurate 3D reconstructed images even for an image matrix of a practical size.

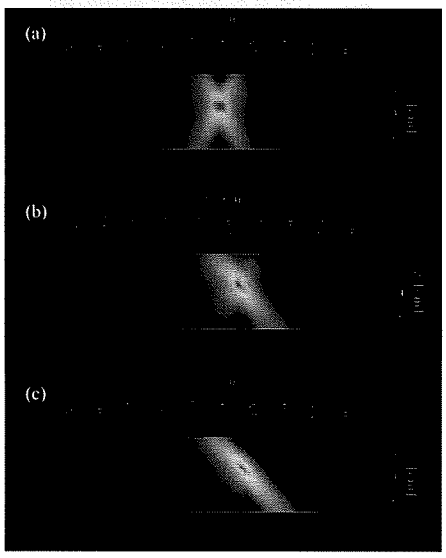

Fig. 1. Position-dependent point-spread functions (PSFs). (a) PSF at x=0 cm; (b) PSF at x=1.2 cm calculated from (a) and (c); (c) PSF at x=2.0 cm.

9781-4244-3962-1/09/$25.00 ©2009 IEEE

III. Results of 3D Tomographic Imaging by Single-Head GREI

In order to confirm the 3D tomographic imaging capability by a single-head GREI, we have performed an imaging experiment with a point-like ^{65}Zn γ-ray source that emits 1115.5 keV γ ray. The source had a columnar shape with diameter and height of 1 mm. Two measurements were performed with the source location of 15 mm and 69 mm away from the detector, respectively. The photopeak counts of 2×10^5 were used for the image reconstruction for each measurement. Fig. 2 shows the results of the imaging experiment. We have succeeded in constructing the 3D images of the point source, and obtained full width at half maximum (FWHM) in XY- and Z-direction of 4 mm and 5 mm for 15-mm away location, and 5 mm and 8 mm for 69-mm away location, respectively.

We applied our 3D tomographic image reconstruction method to the experimental data that was discribed in [1]. Three radioactively labeled tracers of Iodinated (^{131}I) methylnorcholestenol, $^{85}SrCl_2$, and $^{65}ZnCl_2$ were simultaneously administered to a male normal mouse at 8 weeks of age. The mouse had been alive during the imaging experiment.

Fig. 3 shows the results of the 3D tomographic image reconstruction. We were able to visualize the characteristic distribution of each tracers, that is, iodinated (^{131}I) methylnorcholestenol, $^{85}SrCl_2$, and $^{65}ZnCl_2$ accumulated in the adrenal glands, bones, and liver, respectively, and also able to construct hybrid 3D tomographic image that showed the correlation among the tracers.

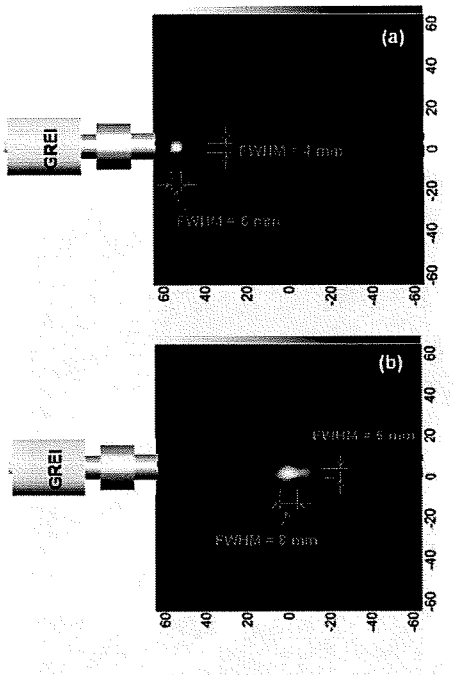

Fig. 2. Maximum intensity projection (MIP) images of the experimental results. The source was located at (a) 15 mm and (b) 69 mm away from the detector. No intensity thresholds were applied in the images.

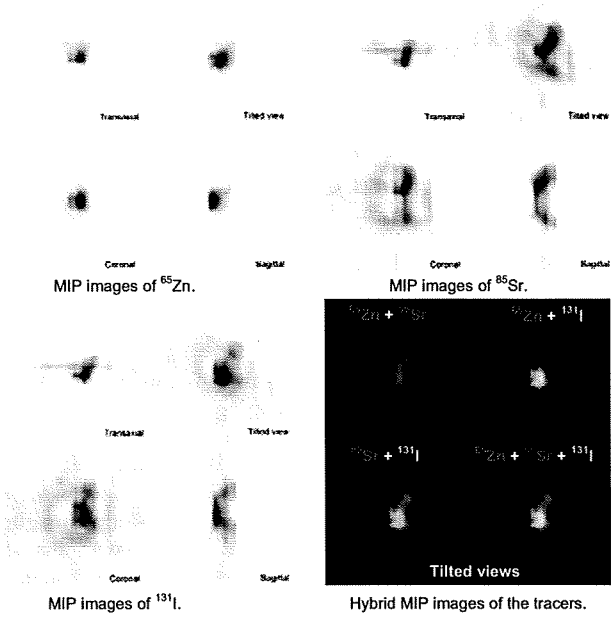

Fig. 3. Results of 3D tomographic image reconstruction. No intensity thresholds were applied in the images

IV. Performance Consideration of Double-Head GREI

We are constructing an array of multiple semiconductor Compton camera units to enlarge the field of view and to obtain more accurate 3D tomographic images. We have evaluated the effect of adding a Compton camera unit by Monte Carlo simulation (Fig. 4). In the simulation, the photopeak counts of 2×10^5 per each camera head were used for the image reconstruction. The results revealed that the response function in Z direction improves to the same value as in X direction if the Compton camera units are positioned in perpendicular direction with respect to the source position. We are expecting FWHM of 1 mm in all directions, once we have constructed a fully-functioning GREI apparatus.

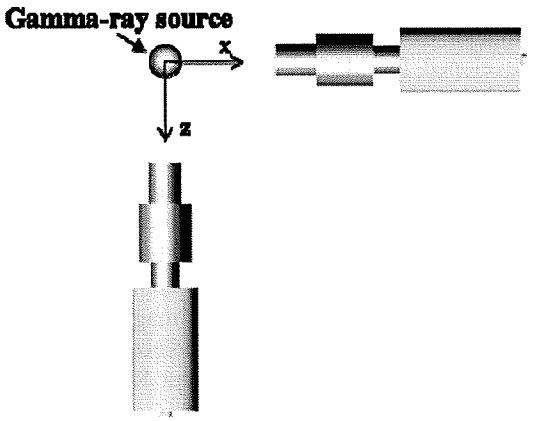

Fig. 4. Two semiconductor Compton camera units positioned in perpendicular direction with respect to the source position.

V. SUMMARY

We are pursuing R&D of multiple molecular simultateous imaging that is an innovative extension of nuclear medical molecular imaging. We have implemented a 3D tomographic image reconstruction method applicable for both single- and multiple-head GREI. In order to enlarge the field of view and to obtain more accurate 3D images, we are constructing a multiple-head GREI system.

ACKNOWLEDGMENT

This research was supported by Molecular Imaging Research Program of Japan's Ministry of Education, Culture, Sports, Science and Technology, Grants-in-aid for Scientific Research of Japan's Ministry of Health, Labor and Welfare, and R&D project of Molecule Imaging Equipment for Malignant Tumor Therapy Support of New Energy and Industrial Technology Development Organization.

REFERENCES

[1] S. Motomura, Y. Kanayama, H. Haba, Y. Watanabe, and S. Enomoto: "Multiple molecular simultaneous imaging in a live mouse using semiconductor Compton camera", *J. Anal. Atom. Spect.* **23**, pp. 1089-1092, 2008.

[2] Shinji Motomura, Shuichi Enomoto, Hiromitsu Haba, Kaori Igarashi, Yasuyuki Gono, and Yasushige Yano, "Gamma-Ray Compton Imaging of Multitracer in Biological Samples Using Strip Germanium Telescope," *IEEE Transactions on Nuclear Science*, **54**, pp. 710-717, 2007.

複数分子同時イメージングの医療応用実現に向けて

医療用コンプトンカメラの開発最前線

本村信治[1] 榎本秀一[1, 2]

1 独立行政法人理化学研究所 分子イメージング科学研究センター メタロミクスイメージング研究ユニット
2 岡山大学 大学院医歯薬学総合研究科 医薬品機能分析学分野

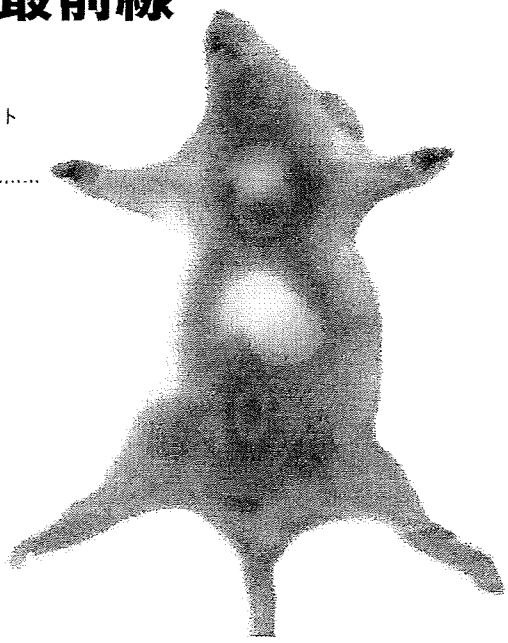

いま日本は，医療用コンプトンカメラの開発で世界をリードしている。そのアイディアが発案されてから30年余り，核医学の分野で，なぜ，いま，コンプトンカメラが注目を浴びているのだろうか。日本発の複数分子同時イメージングで，「Evidence-based Medicine(科学的根拠にもとづく医療)」をめざす，その開発現状を報告する。

複数分子同時イメージングの必要性

近年，遺伝子やタンパク質などの網羅的な解析にもとづき，生命現象の統合的な理解をめざしたオミックス研究*1が盛んにおこなわれ，がんや生活習慣病，脳神経疾患などを含むさまざまな疾患の発症機序や病態の，分子・細胞レベルでの解明が進められている。

分子イメージングの方法論によると，それらの疾患に関与する分子や細胞の，ヒトやその他の生体内における挙動が，定量的な画像情報として取得される。とくに，放射性同位元素（RI, radioisotope）を標識したイメージング剤を用いる核医学の撮像手法は，感度や定量性が高く，投与量が微量で済むため毒性が低いなどの利点があり，ヒトへの適用に適している。2008年6月には厚生労働省より「マイクロドーズ臨床試験の実施に関するガイダンス」*2が発表され，薬理作用や毒性が発現することのない微量の被験物質の投与で薬物動態の情報を評価することが想定されるなど，分子イメージングを適用した創薬・治療・疾患診断研究はいま新たな局面を迎えようとしている。

一般に，疾患の発症機序や病態は1種類の関連分子だけで特徴づけられるわけではなく，複数の因子が複合的に関与することが明らかになってきている。つまり，その疾患を特定的に描出するためには，それら複数の因子それぞれを特異的に観察することのできる複数種の分子プローブを同時に投与して可視化する“複数分子同時イメージング”の実現が望まれる。

しかしながら，現在すでに臨床用分子イメージング診断装置として稼動している陽電子放射断層撮像（PET, positron emission tomography）*3では，一つの波長(エネルギー)のγ線しか撮像できないため，異なる分子プローブを識別するために，異なるエネルギーのγ線を放出するRIを標識して同時に撮像するということができない。また，γ線の撮像のために機械的なコリメータ*4を必要とする単光子放射断層撮像（SPECT, single photon emission computed tomography）*5では，撮像可

FOOTNOTE

*1 オミックス研究
ある生命現象に関与する物質を網羅的に解析し，それらを統合することでその生命現象を解明することを目的とした研究。着目する対象が遺伝子の場合はゲノミクス（Genomics），タンパク質の場合はプロテオミクス（Proteomics）など，いくつかの階層が考えられ，英文表記ではオミックス(-omics)が接尾辞となっている。

*2 「マイクロドーズ臨床試験の実施に関するガイダンス」
医薬食品局発出の平成20年6月3日付薬食審査発第0603001号。厚生労働省「治験」ホームページより；http://www.mhlw.go.jp/topics/bukyoku/isei/chiken/dl/080705.pdf 有効で安全な医薬品を迅速に提供することを目的として臨床試験の初期段階でおこなわれる，微量の被験物質の投与による薬物動態などの評価に関する指針が示された。

図1 コンプトンカメラの撮像原理

コンプトン散乱事象を一つ検出すると，コンプトン散乱の方程式を解いてその散乱角度が求められ，図中の円錐上のどこかにγ線源が存在することがわかる。このような円錐の情報を多数集めるとγ線源の場所が特定でき，たとえば薬剤の分布画像を推定することが可能となる。

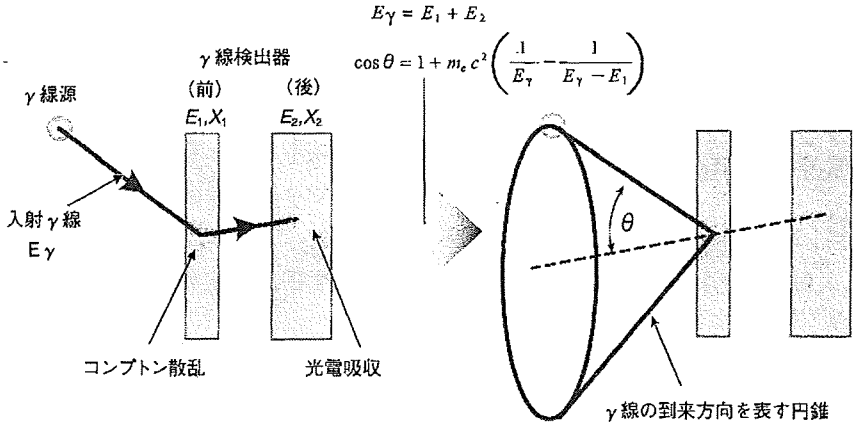

図2 撮像可能なγ線のエネルギー範囲

コンプトンカメラはPETやSPECTに比べて格段に広いエネルギー範囲のγ線を撮像することが可能であるため，標識に利用可能な核種の選択肢が格段に増え，代謝安定性や標的事象のタイムスケールを考慮した標識化が可能になる。

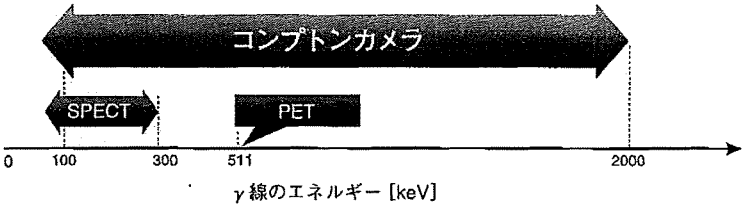

能なγ線が低エネルギーの領域に限られるため，分子プローブの標識に利用可能なRIが制限される。そのため，これまでに核医学における複数分子同時イメージングの優位性を議論の対象とした研究はほとんどおこなわれていないのが現状である。

『コンプトンカメラとは？』

1923年にアーサー・コンプトンによって確かめられた，光（電磁波）と電子の相互作用による散乱現象を「コンプトン散乱」とよぶ。散乱前の光のもつエネルギーが既知であれば，散乱の角度により，散乱後の光および電子のもつエネルギーは，運動学的に一意に決定できるというもの。光の粒子性を示す現象の一つである。
この現象を利用した撮像装置が「コンプトンカメラ」である。γ線のコンプトン散乱がおこると，散乱後のγ線はその散乱角度に対応して連続的にエネルギーが変化する。これを利用して，そのエネルギーの変化から散乱角度を推定し，γ線放出RIを標識した薬剤の分布像を取得する。図1にみるように，複数の半導体検出器などを並べることによって実現される。

複数分子同時イメージングを実現するコンプトンカメラ

筆者らは，分子イメージング診断装置として“コンプトンカメラ（コンプトン散乱の運動学を利用して，γ線源の密度分布を画像化する装置；囲み参照）”を用いることで，複数分子同時イメージングが実現可能であることを提案し，生きたままのマウスの撮像実験でこれを実証することに世界で初めて成功した[1, 2]。この複数分子同時イメージングは日本発のアイディアであり，いま医療用コンプトンカメラの研究開発の分野においてはわが国が世界をリードしている。

コンプトンカメラのアイディアはすでに1970年代初頭にγ線天文学*6用の観測装置として提案されており[3]，その後すぐに医用画像化診断装置としても提案されていた[4]。それからもさまざまなタイプのコンプトンカメラが提案されたが[5]，未だに医用画像化診断装置として実用化された例はない。この理由としては，これまで既存のPETやSPECTに対して顕著な優位性を示すことができていなかったためであると考えられる。しかし生命科学の進歩は，複数分子の同時画像化分析をここにきて強く要求する段階に至った。一方で，放射線検出技術や情報処理技術の進歩がその要求に応えられるであろうことが明らかになってきた今日，医療用コンプトンカメラをいち

FOOTNOTE

*3 陽電子放射断層撮像（PET）
陽電子を放出する種類のRIを標識に用い，その陽電子が消滅する際に180°の角度相関をもって放出される2本の511 keVのγ線を，被検体の周囲に配置した対向する放射線検出器で検出することで，薬剤の分布像を撮像可能にする装置。感度や定量性が高く，分子イメージングの主要な技術として位置づけられている。

早く実用化することで，医用画像化診断装置の分野にもブレークスルーがもたらされることが期待される。

コンプトンカメラの撮像原理と特徴

コンプトンカメラの撮像原理は，センサーに入射したγ線のコンプトン散乱現象をとらえることである（図1）。可視光の場合の散乱とはちがい，コンプトン散乱後のγ線はその散乱角度に応じてエネルギーが連続的に変化する。このエネルギーを精度よく測定することでγ線の散乱角度を求めることができ，この情報からγ線の入射方向を表す円錐が定められる。そして，検出した一つ一つのコンプトン散乱事象に対して決定された円錐の情報を多数集めて演算処理することで，γ線源の分布像を推定することが可能となる。

このように，コンプトンカメラには機械的なコリメータ*4が不要であるため，コリメーションによる感度の低下*4がなく，既存のPETやSPECTに比べて格段に広いエネルギー範囲のγ線を撮像することが可能である（図2）。さらに，機械的なコリメータによるγ線入射方向の制限がなく，1台のカメラユニットに対してさまざまな角度で入射したγ線を捉えることができる。このため，一方向からの固定撮像でもγ線源の分布像を複数の方向へ投影した3次元の情報が得られるという特徴を有する。そして，エネルギー分解能*7が

図3 理化学研究所の半導体コンプトンカメラ「GREI」[1, 2]

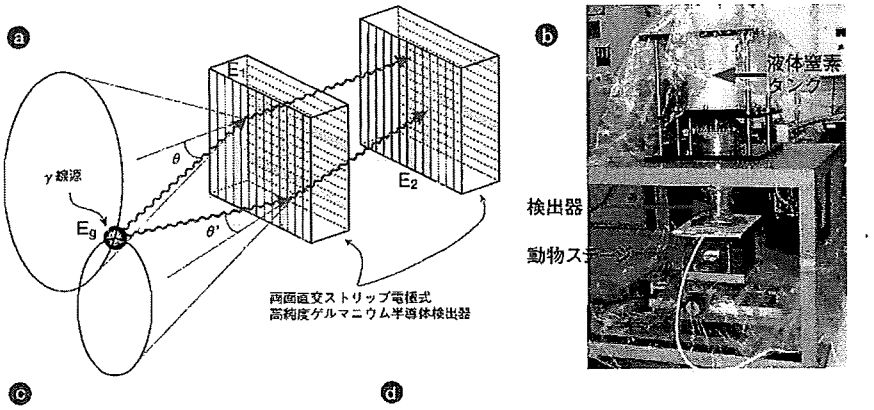

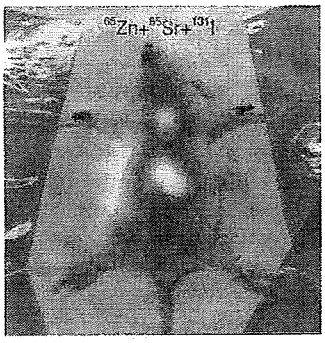

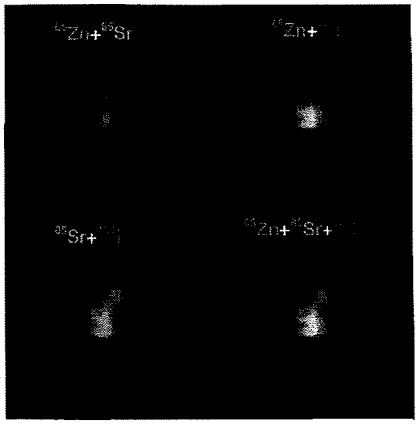

(a) GREIの概念図。前後の検出器（センサー）は両面直交ストリップ電極式高純度ゲルマニウム（Ge）半導体であり，入射γ線の相互作用位置とエネルギーを高精度に測定できる。
(b) GREIのプロトタイプ。
(c) GREIで同時撮像した3種類の放射性薬剤の複合画像。ヨウ化メチルノルコレステノール（^{131}I）注射液（^{131}I-Adosterol），塩化ストロンチウム（$^{85}SrCl_2$），塩化亜鉛（$^{65}ZnCl_2$）をマウスに同時投与し，生きたままそれぞれの薬剤の挙動のちがいを画像化することに成功した。（文献[2]より許可を得て転載）
(d) GREIで同時撮像した3種類の放射性薬剤の3次元断層画像。図3cの撮像実験で得られたデータを演算処理して画像化した。被検体をGREIで1方向から撮像しただけで，それぞれの薬剤の3次元分布の情報が得られた。（文献[2]より許可を得て転載）
(e) 3種類の放射性薬剤の複合的3次元断層画像。図3dの画像を薬剤ごとに色分けし，それらを組み合わせて画像生成した。組合せを変えて表示することで，それぞれの薬剤の相互作用などを視覚的に表示することが可能になる。

*4 コリメータ，コリメーションによる感度の低下
コリメータは，鉛など原子番号が大きく密度が高い物質を素材とし，放射線検出器の前面に設置してγ線などの検出器への入射方向を制限するように穴加工が施された部材。
γ線源からあらゆる方向にγ線が放出されるが，コリメータの穴を通過したγ線だけしか検出できず，その穴の方向に対する投影画像のみ得ることができる。したがって，その他の方向に入射して検出されなかったγ線の情報は利用できないため，感度の低下は避けられない。また，γ線のエネルギーが約300 keV以上になると，透過や散乱の確率が高くなり，コリメータの有効性は低下する。

図4 宇宙航空研究開発機構(JAXA)のSi/CdTeコンプトンカメラ[7]

ⓐ Si/CdTeコンプトンカメラの概念図

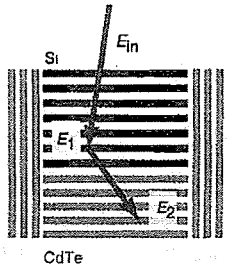

ⓑ-1 両面Siストリップ検出器

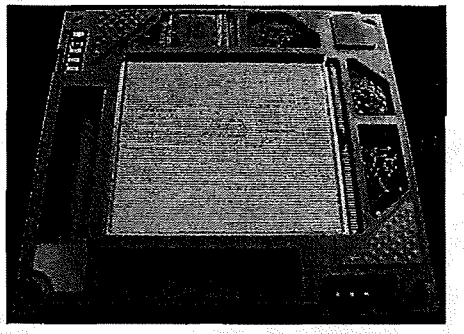

ⓑ-2 積層型・両面Siストリップ検出器

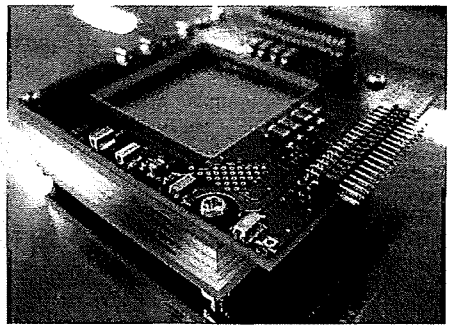

ⓑ-3 大面積・両面CdTeストリップ検出器

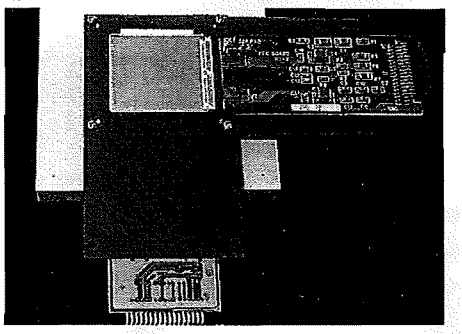

ⓒ 医療用Si/CdTeコンプトンカメラのプロトタイプ

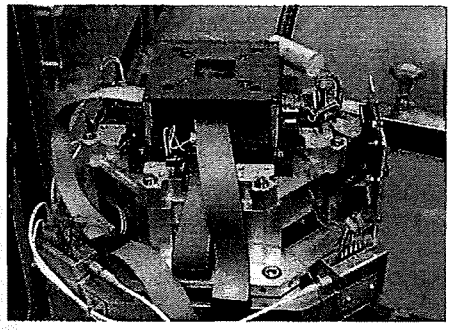

(a) Si/CdTeコンプトンカメラの概念図。SiおよびCdTe半導体は常温でも放射線検出器として作動させることが可能なため，大掛りな冷却装置が不要で，コンパクトな撮像装置の構築が可能である。
(b) b-1は両面Siストリップ検出器，b-2は積層型・両面Siストリップ検出器，b-3は大面積・両面CdTeストリップ検出器。人工衛星に搭載し，宇宙空間における過酷な条件下で使用するために開発されたこれらの技術が，いま医療用画像診断装置に展開されようとしている。
(c) 医療用Si/CdTeコンプトンカメラのプロトタイプ。コンパクトに構築されており，局部の近接撮像が可能である。(写真はJAXA・高橋忠幸教授のご厚意による)

優れたセンサーを用いれば，異なる因子に対する分子プローブそれぞれに対して異なるエネルギーのγ線を放出するRIを標識することで，複数分子同時イメージングが可能になるのだ。

わが国における医療用コンプトンカメラ研究開発プロジェクト

筆者らが実用化に向けて開発中のコンプトンカメラは，センサーとして両面直交ストリップ電極式[*8]ゲルマニウム（Ge）半導体検出器を用いた半導体コンプトンカメラで，gamma-ray emission imaging にちなんで『GREI』と称している（図3）。Ge半導体検出器は，半導体検出器としては，単結晶で大体積の放射線検出器が作製可能で，エネルギー分解能がきわめて優れており，コンプトンカメラの素材として非常に適した性質をもっている。また使用した検出器は，信号を読み出すための電極が短冊状に分割されているため，検出器内のどこで入射γ線の相互作用がおこったかを検出することができるようになっている。

前述の通り，筆者らはすでに複数分子同時イメージングの実証に成功しているが[2, 6]，現在のGREIのプロトタイプを用いた典型的な撮像実験では，約5 mmの空間解像度の画像を得るために10時間程度の撮像時間を要しており、まだ実用的とは言い難いのが現状である。そこで，現在さらなる画質の向上と撮像時間の短縮をめざし，GREIに実装される要素技術の高度化開発をおこなっている。具体的な開発項目には，①γ線の検出信号解析法の高度化による相互作用位置検出精度の向上，γ線トラッキング法[*9]の実装，②高精度3次元画像再構成法の開発，③低エネルギーγ線撮像法の開発，などが含まれる。このような要素技術の高度化を達成し，1時間以内の撮像でサブミリオーダーの空間解像度の画像化を可能にすることを目標にしている。

日本では筆者ら以外にも，大きく分けて二つのグループが医療用コンプトンカメラの研究開発を推進している。宇宙航空研究開発機構（JAXA）

FOOTNOTE

*5 単光子放射断層撮像(SPECT)
コリメータを装備したγ線検出器を用いて，被検体の周囲の複数の方向から撮像したデータを演算処理した像，γ線放出RIを標識した薬剤の分布像を取得する装置。

*6 γ線天文学
地球外の天体などから放出されるγ線を観測することで，宇宙におけるさまざまな物理現象の解明を目的とした研究分野。とくに1 MeV前後のγ線に対しては，もっとも高感度の観測装置としてコンプトンカメラが用いられている。

*7 エネルギー分解能
エネルギー値の異なる二つの放射線について，どのくらいの差まで区別して測定できるかという能力をいう。エネルギー分解能が高いと，分子プローブの識別能が向上するだけでなく，γ線の散乱角の推定精度も向上するため，コンプトンカメラにとってはとくに重要な要因である。

図5 京都大学の電子飛跡検出型コンプトンカメラ[8]

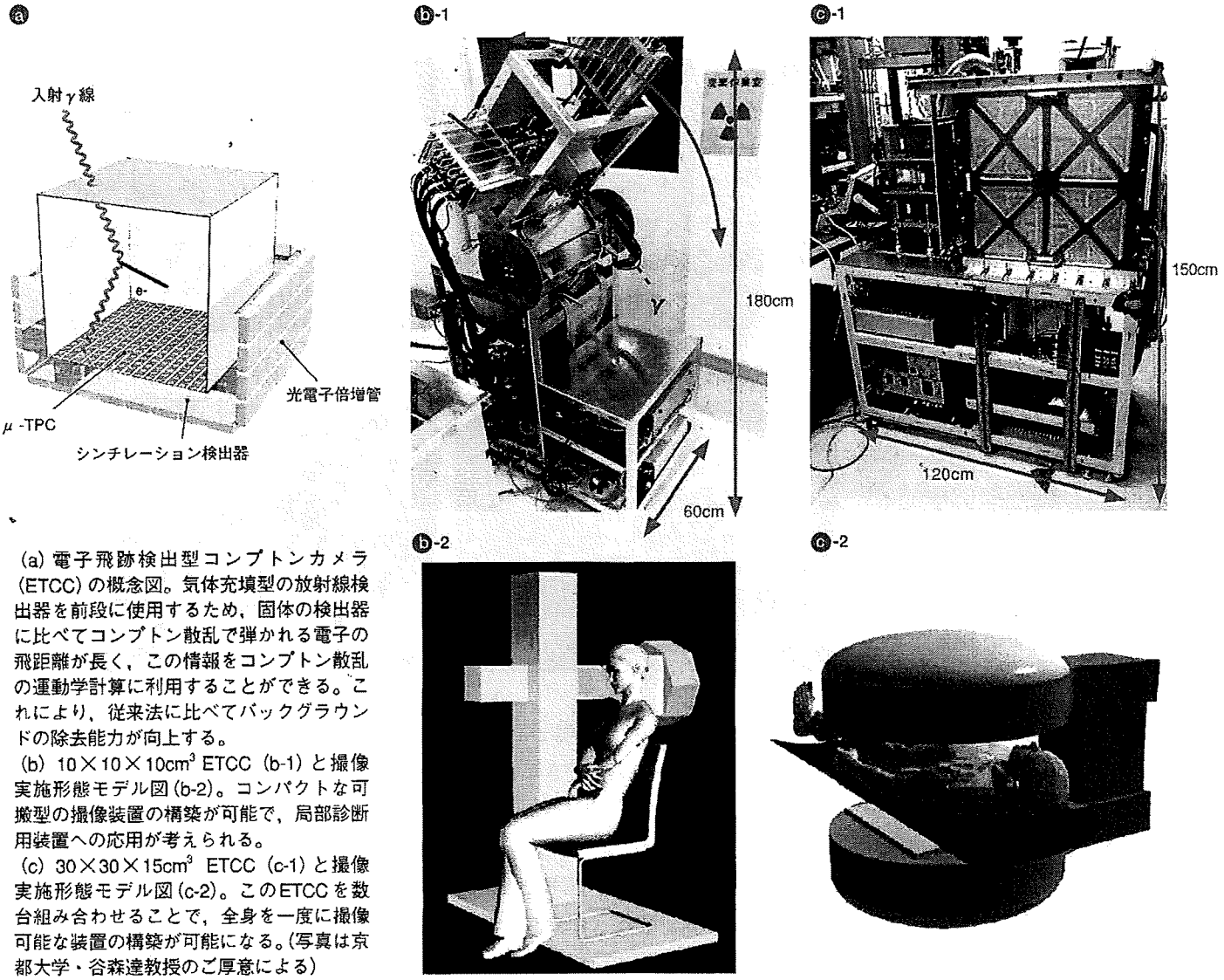

(a) 電子飛跡検出型コンプトンカメラ(ETCC)の概念図。気体充填型の放射線検出器を前段に使用するため，固体の検出器に比べてコンプトン散乱で弾かれる電子の飛距離が長く，この情報をコンプトン散乱の運動学計算に利用することができる。これにより，従来法に比べてバックグラウンドの除去能力が向上する。
(b) 10×10×10cm^3 ETCC (b-1) と撮像実施形態モデル図(b-2)。コンパクトな可搬型の撮像装置の構築が可能で，局部診断用装置への応用が考えられる。
(c) 30×30×15cm^3 ETCC (c-1) と撮像実施形態モデル図(c-2)。このETCCを数台組み合わせることで，全身を一度に撮像可能な装置の構築が可能になる。(写真は京都大学・谷森達教授のご厚意による)

の高橋忠幸教授らの研究グループは，センサーとしてシリコン (Si) およびテルル化カドミウム (CdTe) *10半導体検出器を組み合わせたSi/CdTeコンプトンカメラの開発をおこなっている[6](図4)。この装置はGREIと同じく半導体コンプトンカメラの範疇に入るが，高性能半導体センサー技術，低雑音アナログ信号処理LSI技術，高密度実装技術など，高度な衛星搭載機器開発技術が導入されており，同グループは，Si/CdTeコンプトンカメラによるγ線イメージングを世界に先駆けて実証することに成功している。SiやCdTeは常温でも動作する半導体検出器であり，GREIに比べてコンパクトな実装が可能になるため，可搬型コンプトンカメラとしての位置づけが期待される。すでに筆者らのグループと共同して小動物の撮像実験による実証にも成功しており，現在さらなる小型化・高性能化をめざして高度実装技術の導入が進められている。

*8 両面直交ストリップ電極式
平板型の半導体放射線検出器の両面には，検出信号を取り出すための電極加工が施されている。その両面の電極を互いに直交する方向の短冊(ストリップ)状に分割すれば，両面の電極位置の組み合わせでγ線の相互作用位置の検出が可能になる。

*9 γ線トラッキング法
一つのγ線検出器内で複数回の相互作用がおこった場合に，コンプトン散乱の運動学などの情報を駆使し，その相互作用の順序を導出する手法。計測データだけではそれらの順序を決定できないため無効なデータとなってしまうが，この手法を用いるとそれらを有効なデータとして取り込むことが可能になり，感度を向上させることができる。

京都大学の谷森達教授らの研究グループは，ある種のガスを封入したμ-TPC(Micro pixcel chamber mounted Time Projection Chamber) とよばれる放射線検出器とシンチレーション検出器*11を組み合わせた電子飛跡検出型コンプトンカメラ (Electron Tracking Compton Camera, ETCC) の開発をおこなっている[7](図5)。μ-TPCは，入射γ線のコンプトン散乱の際に弾き飛ばされる電子の飛跡を検出可能であり，通常のコンプトンカメラでは円錐状にしか定まらないγ線の到来方向をさらに円錐の一部の領域に絞り込むことができ，バックグラウンドの除去能力に優れている。また，広視野の装置が比較的安価に構築できるという利点があるため，複数検出ヘッドの装置開発なども率先しておこなわれており，全身撮像用コンプトンカメラの実現が期待される。μ-TPCのようなガス充填型検出器は，半導体コンプトンカメラに比べるとエネルギー分解能が劣るためRIの識別能力は見劣りするが，3種類程度のRIの同時撮像には成功しており，複数分子同時イメージングも可能であろうと期待される。

ここに紹介した三つの研究グループは，医療用コンプトンカメラ開発に関するオールジャパンコンソーシアムの中心的役割を担っていくことが期待されている。今後もより連携体制を強化し，欧米諸国に対する日本のリーダーシップを維持していきたいと考えている。

新たな創薬・疾患診断法の創出に向けた課題

これまで複数分子同時イメージングの機器開発に関する話題を中心に述べてきたが，この手法が成功するためには，ある疾患の発症機序や病態をもっとも顕著に特徴づける複数の因子を探しだす必要がある。PET用の分子プローブはそのままGREIでも撮像可能であるため，筆者らの研究グループでは，まず候補となる抗体やペプチドを用いたプローブの生体内動態を一つひとつ小動物用PETで調べ，その後，GREIによる撮像実験で検証する方法で検討が進められている。それらの候補物質の標識にGREI用のRIを用いれば，複数分子同時イメージングが可能になるという訳である。ただし，それらの候補因子をシステマティックに探索する手法はまだ確立されていない。

近年，異なる階層のオミックス研究*1の成果を結合し，生命のメカニズムの統合的な理解をめざした，システムバイオロジーの確立に向けた研究が盛んにおこなわれている。このシステムバイオロジーの成果を利用できれば，遺伝子多型などの個体差の情報も考慮した効果的な疾患関連因子の探索も可能になるかもしれない。

しかしながら，この疾患関連因子の探索を実現するには，大規模な代謝ネットワークの解析など，膨大な量の演算処理が必要になると予想される。また，候補因子の探索ができたとしても，それらを特異的に描出できる分子プローブの設計・合成が必要である。これらの実施を可能にする基盤としては，次世代スーパーコンピュータの整備や，研究機関や分野の垣根を越えた研究協力体制の実現が求められるであろう。にわかに実現することは困難かもしれないが，オールジャパンの研究体制による，真の「Evidence-based Medicine (科学的根拠にもとづく医療)」の実現に期待したい。

Profile

もとむら・しんじ
理化学研究所 神戸研究所 分子イメージング科学研究センター メタロミクスイメージング研究ユニット 研究員。
2002年，九州大学大学院理学研究科博士後期課程を単位取得のうえ退学。2003年，同大学より博士(理学)の学位を取得。理化学研究所基礎科学特別研究員などを経て，2008年10月から現職。次世代・複数分子同時イメージングをめざしたコンプトンカメラの高度化開発に従事。

えのもと・しゅういち
岡山大学 大学院医歯薬学総合研究科 医薬品機能分析学分野 教授。理化学研究所 神戸研究所 分子イメージング科学研究センター メタロミクスイメージング研究ユニット 研究ユニットリーダー。
1991年北海道大学大学院薬学研究科博士後期課程修了，薬学博士。日本学術振興会PD，理化学研究所基礎科学特別研究員，理化学研究所仁科加速器研究センター副チームリーダーなどを経て，2008年10月から現職。メタロミクス研究と分子イメージング研究を推進中。

参考文献

[1] Motomura S et al:IEEE Trans Nucl Sci 54(2007) 710-717
[2] Motomura S et al:J Anal Atom Spectrom 23(2008) 1089-1092
[3] Schönfelder V et al:Nucl Instrum Methods 107(1973) 385-394
[4] Todd R W et al:Nature 251(1974) 132-134
[5] Phillips G W:Nucl Instrum Methods Phys Res B 99(1995) 674-677
[6] 榎本秀一:Medical Bio 2008年11月号(2008) 14-15
[7] Watanabe S et al:Nucl Instrum Methods A 579(2007) 871-877
[8] Kabuki S et al:Nucl Instrum Methods A 580(2007) 1031-1035

FOOTNOTE

*10 テルル化カドミウム
半導体としての性質をもつ，CdとTeの化合物。Si半導体と同様に，常温で作動可能な半導体放射線検出器の素材として利用されている。

*11 シンチレーション検出器
放射線との相互作用で発光(シンチレーション)する物質を素材とした放射線検出器。

Toxicology and Applied Pharmacology 241 (2009) 195–201

Contents lists available at ScienceDirect

Toxicology and Applied Pharmacology

journal homepage: www.elsevier.com/locate/ytaap

Involvement of DNA hypermethylation in down-regulation of the zinc transporter ZIP8 in cadmium-resistant metallothionein-null cells

Hitomi Fujishiro [a], Satomi Okugaki [a], Saori Yasumitsu [a], Shuichi Enomoto [b,c], Seiichiro Himeno [a,*]

[a] Laboratory of Molecular Nutrition and Toxicology, Faculty of Pharmaceutical Sciences, Tokushima Bunri University, Yamashiro-cho, Tokushima 770-8514, Japan
[b] Metallomics Imaging Research Unit, Center for Molecular Imaging Science, RIKEN Kobe Institute, Minatojima-minamimachi, Chuo-ku, Kobe, Hyogo 650-0047, Japan
[c] Department of Pharmaceutical Analytical Chemistry, Graduate School of Medicine, Dentistry and Pharmaceutical Sciences, Okayama University, Tsushima-naka, Kita-ku, Okayama, 700-8530, Japan

ARTICLE INFO

Article history:
Received 11 May 2009
Revised 31 July 2009
Accepted 13 August 2009
Available online 20 August 2009

Keywords:
Cadmium
Zinc
Transport
Resistance
DNA hypermethylation
Epigenetics

ABSTRACT

The Zrt/Irt-related protein 8 (ZIP8) encoded by *slc39a8* is now emerging as an important zinc transporter involved in cellular cadmium incorporation. We have previously shown that mRNA and protein levels of ZIP8 were decreased in cadmium-resistant metallothionein-null (A7) cells, leading to a decrease in cadmium accumulation. However, the mechanism by which ZIP8 expression is suppressed in these cells remains to be elucidated. In the present study, we investigated the possibility that epigenetic silencing of the *slc39a8* gene by DNA hypermethylation is involved in the down-regulation of ZIP8 expression. A7 cells showed a higher mRNA level of DNA methyltransferase 3b than parental cells. Hypermethylation of the CpG island of the *slc39a8* gene was detected in A7 cells. Treatment of A7 cells with 5-aza-deoxycytidine, an inhibitor of DNA methyltransferase, caused demethylation of the CpG island of the *slc39a8* gene and enhancement of mRNA and protein levels of ZIP8. In response to the recovery of ZIP8 expression, A7 cells treated with 5-aza-deoxycytidine showed an increase in cadmium accumulation and consequently an increase in sensitivity to cadmium. These results suggest that epigenetic silencing of the *slc39a8* gene by DNA hypermethylation plays an important role in the down-regulation of ZIP8 in cadmium-resistant metallothionein-null cells.

Introduction

Recent progress in the research field of metal transporters has provided new insights into the cellular transport mechanism of cadmium in mammalian cells. Since cadmium is not an essential metal, the cell entry pathways of other essential metals are utilized for cellular cadmium incorporation. To date, a variety of transport systems for iron, calcium, and zinc have been shown to be involved in cadmium uptake. Earlier studies have shown that intestinal absorption of cadmium was increased by dietary deficiency of iron (Valberg et al., 1976) or calcium (Washko and Cousins, 1977), and these effects are now attributed to the enhanced expression of divalent metal transporter 1 (DMT1), a ferrous iron transporter (Gunshin et al., 1997), or calcium transporter 1 (CAT1), an intestine-specific calcium transporter (Min et al., 2008), respectively, in the intestine.

Recently, Dalton et al. (2005) have identified *slc39a8*, which encodes a zinc transporter, the Zrt/Irt-related protein 8 (ZIP8), as a gene responsible for the genetic difference in cadmium-induced testicular hemorrhage among inbred mouse strains. Ectopic expression of ZIP8 in mouse fetal fibroblast cells, MDCK cells, and *Xenopus* oocytes (Dalton et al., 2005; He et al., 2006; Liu et al., 2007) resulted in an increase in cadmium uptake. Furthermore, ZIP8 transgenic mice exhibited severe damages in the testis and kidney when treated with $CdCl_2$ at a dose not causing damages in wild-type mice (Wang et al., 2007). These studies suggest that the zinc transporter ZIP8 plays an important role in the transport of cadmium in the testis and kidney, the target organs of cadmium toxicity *in vivo*.

Previously, we established cadmium-resistant cells from metallothionein (MT)-null mouse fibroblast cells and showed that cadmium uptake in these cells is markedly suppressed (Yanagiya et al., 1999; Yanagiya et al., 2000). This cell line was the first in which cadmium resistance was conferred by reduced accumulation of cadmium and provided a good tool for clarifying cadmium transport system (Himeno, 2002; Himeno et al., 2009). By using a DNA microarray (Fujishiro et al., 2006) and subsequent real-time PCR assays (Fujishiro et al., 2009), we found that the expression of ZIP8 at both the mRNA and protein levels was markedly down-regulated in cadmium-resistant MT-null cells. In addition, introduction of shRNA of ZIP8 into parental cells resulted in a decrease in cadmium accumulation (Fujishiro et al., 2009). These data suggest that the down-regulation of ZIP8 plays a pivotal role in the decrease in cadmium accumulation and subsequent acquisition of cadmium resistance in MT-null cadmium-resistant cells. However, the reason for the decrease in ZIP8 mRNA levels in these cells remains unclear.

Abbreviations: ZIP8, Zrt/Irt-related protein 8; MT, metallothionein; GCLC, glutamate cysteine ligase catalytic; 5-aza-dC, 5-aza-deoxycytidine; DNMT, DNA methyltransferase; MSP, methylation-specific PCR; 5′-NT, ecto-5′-nucleotidase.

* Corresponding author. Fax: +81 88 655 3051.
E-mail address: himenos@ph.bunri-u.ac.jp (S. Himeno).

0041-008X/$ – see front matter © 2009 Elsevier Inc. All rights reserved.
doi:10.1016/j.taap.2009.08.015

To date, few studies have examined the mechanisms of transcriptional regulation of the *slc39a8* gene. A recent study reported the involvement of Sp1 in the down-regulation of the *slc39a8* gene in the human lung cancer cell line SR3A which was stably transfected with the glutamate cysteine ligase catalytic (GCLC) subunit (Aiba et al., 2008). On the other hand, several studies have demonstrated that DNA methylation was facilitated by long-term exposure to cadmium (Takiguchi et al., 2003; Benbrahim-Tallaa et al., 2007; Jiang et al., 2008). Since hypermethylation of DNA plays a critical role in the epigenetic silencing of gene expression, we focused on the possibility that hypermethylation of the *slc39a8* gene is involved in the repression of ZIP8 expression in MT-null cadmium-resistant cells. For this purpose, we examined the effects of 5-aza-deoxycytidine (5-aza-dC), an inhibitor of DNA methyltransferase (DNMT), on ZIP8 expression in cadmium-resistant cells and compared the methylation status of the *slc39a8* gene between cadmium-resistant and parental cells. Here we show that the down-regulation of ZIP8 in MT-null cadmium-resistant cells was caused, at least partly, by hypermethylation of the *slc39a8* gene. Our results provide evidence that epigenetic silencing of a metal transporter gene plays a significant role in the acquisition of resistance against a toxic metal.

Materials and methods

Materials. [^{109}Cd]-$CdCl_2$ was produced by using the RIKEN AVF cyclotron in Japan as described previously (Haba and Enomoto, 2005) and was purified by an ion exchange system (Kraus and Nelson, 1955). Rabbit anti-Sp1 polyclonal antibody and rabbit anti-ecto-5′-nucleotidase (5′-NT) polyclonal antibody were purchased from Santa Cruz Biotechnology (Santa Cruz, CA).

Cell culture. Cadmium-resistant MT-null cells (A7) and parental (P) cells were established previously from MT-null mouse embryonic fibroblasts (Yanagiya et al., 1999). A7 and P cells were cultured in Dulbecco's modified Eagle's medium (DMEM) supplemented with 10% fetal bovine serum (FBS), penicillin, and streptomycin under 5% CO_2 at 37°C. The media were changed every 3–4 days.

Electrophoretic mobility shift assay. The electrophoretic mobility shift assay (EMSA) and extraction of cell nuclei were carried out as described previously (Donai et al., 2001). The oligonucleotide probe with the consensus Sp1 binding site, 5′-ATT CGA TCG GGG CGG GGC GAG C -3′, was purchased from Promega (Madison, WI) and end-labeled with [γ-^{32}P]ATP (Perkin-Elmer, Inc., Boston, MA) by using T4 polynucleotide kinase (TOYOBO, Co., Osaka, Japan). The binding reaction was carried out in a reaction mixture containing 0.3 μg/μl poly(dI–dC) (Sigma-Aldrich), 10% glycerol, 20 mM HEPES buffer (pH 7.9), 50 mM KCl, 0.5 mM dithiothreitol (DTT), 3 μg of the nuclear extract, 0.5 mM phenylmethylsulfonyl fluoride (PMSF), 0.5 mM EDTA, and 0.5 ng of ^{32}P-labeled probe. In the supershift assay, 1.0 μg of anti-Sp1 antibody was added to the reaction mixture. In the competition experiment, 10-fold molar excess of unlabeled oligonucleotide was incubated with the nuclear extracts for 20 min at room temperature before the addition of ^{32}P-labeled oligonucleotide. After incubation for 20 min with ^{32}P-labeled probe, the reaction mixture was electrophoresed on 8% polyacrylamide gel, fixed, and dried. The band shifts were visualized by FLA2000G (Fuji photo Film Co., Ltd., Kanagawa, Japan).

Treatment of cells with 5-aza-2′-deoxycytidine. Cells were seeded at a density of 1×10^6 cells per 100 mm dish, preincubated for 24 h, and then cultured in medium containing 10 μM 5-aza-dC (Sigma-Aldrich, St. Louis, MO) for 72 h. The medium containing 5-aza-dC was exchanged for fresh medium every 24 h. Twenty-four hours after the last addition of 5-aza-dC to the media, cells were washed with phosphate-buffered saline (PBS) and used for the extraction of genomic DNA, total RNA, and membrane fractions for the following experiments.

DNMT activity. The nuclear lysates from A7 and P cells were obtained by using EpiQuik Nuclear Extraction Kit I (Epigentek Group, New York, NY) and analyzed for total DNMT activity by using EpiQuik DNA Methyltransferase Activity Assay Kit (Epigentek Group, New York, NY) according to the manufacturer's instruction. The enzyme activity (absorbance at 450 nm/h/mg protein) of A7 cells was expressed as relative ratio to that of P cells.

Preparation of RNA and RT–PCR. Total RNA was extracted and purified from cells using an SV Total RNA Isolation System (Promega). The reverse transcription (RT) reaction was performed in a mixture containing 50 mM Tris–HCl (pH 8.3), 70 mM KCl, 3 mM $MgCl_2$, 10 mM DTT, 1 mM each dNTPs, 4 U of RNase inhibitor, 2 μg of total RNA, 0.5 μM Oligo$(dT)_{15}$ primer, and 5 U of reverse transcriptase in a total volume of 20 μl. PCR was performed in a solution containing 10 mM Tris–HCl (pH 8.3), 50 mM KCl, 1.5 mM $MgCl_2$, 1 U of Taq DNA polymerase, 0.4 μM upstream and downstream primers, and an aliquot of the RT reaction mixture. The amplification profile was an initial denaturation at 94 °C for 2 min, then 25–30 cycles of denaturation at 98°C for 20 sec, annealing at 56–58°C for 1 min, and extension at 72°C for 1 min. An automated DNA thermal cycler (TaKaRa Bio Inc., Shiga, Japan) was used. The following oligonucleotides were used for RT–PCR: as ZIP8 primers of 5′ sense and 3′ antisense, 5′-TCCCTGCGAGGATCTAAGAA-3′ and 5′-AGCGAGTCCCACGAAATAAG-3′; as DNMT1 primers of 5′ sense and 3′ antisense, 5′-CGGCCAACCTGGAGAGCA-3′ and 5′-CCAGTTTCTCCACAGCAGC-3′; as DNMT3a primers of 5′ sense and 3′ antisense, 5′-CACACAGAAGCATATCCAGGAGTG-3′ and 5′-AGTGGACGGGGAAGCCAAACACCC-3′; and as DNMT3b primers of 5′ sense and 3′ antisense, 5′-AACGTCAATCCTGCCCGCAAAGGT-3′ and 5′-ACTGGGTTACATGCCAGGAATCTT-3′, β-actin primers of 5′ sense and 3′ antisense; 5′-CATGGATGACGATATCGCT-3′ and 5′-CATGAGGTAGTCTGTCAGGT-3′, respectively. PCR fragments were analyzed by electrophoresis on a 1.5% agarose gel.

Immunoblot analysis. Cells were harvested after washing with PBS, and then sonicated in 100 μl of extraction buffer. The extraction buffer consisted of 40 mM Tris–HCl (pH 7.6), 1 mM DTT, 1 mM EGTA, 10% glycerol, 1 mM PMSF, and 5.5% protease inhibitor cocktail (Sigma-Aldrich). After centrifugation at $18{,}500 \times g$ for 30 min, the precipitation fraction was used as a membrane fraction. Proteins were separated by 10% SDS–polyacrylamide gel electrophoresis and electrophoretically transferred to a PVDF membrane. The transblot was preincubated with 5% non-fat dry skim milk in Tris-buffered saline (TBS; pH 7.4) and then incubated with anti-ZIP8 antibody (1:1000) or anti-5′-NT antibody (1:200) overnight (Fujishiro et al., 2009). The membrane was washed with TBS–0.05% Tween 20, and then incubated with horseradish peroxidase-coupled goat anti-rabbit IgG (Sigma-Aldrich) antibody (1:3000). After the membrane was washed with TBS–0.05% Tween 20, the immunoreactive bands were detected using enhanced chemiluminescence reagents.

Measurement of cellular cadmium accumulation. For the measurement of cadmium accumulation, A7 and P cells treated with 5-aza-dC were cultured in drug-free media for 2 h and then cultured in serum-free media containing 1.0 μM [^{109}Cd]-labeled $CdCl_2$ for 1 and 18 h at 37 °C. After washing three times with 0.5 ml of ice-cold medium containing FBS followed by washing with PBS containing 0.05% EDTA, the cells were harvested with 1.0 ml PBS containing 0.5% trypsin/EDTA, and transferred to a test tube. The radioactivity of ^{109}Cd was measured with an auto-well gamma counter (ARC-300; Aloka, Tokyo, Japan). All experiments were carried out three times and an average value was used.

Assay for sensitivity to cadmium. 5-Aza-dC-treated and untreated A7 cells and untreated P cells were plated on 96-well microplates at a density of 2×10^4 cells per well, incubated for 24 h in drug-free media,

and then treated with various concentrations of $CdCl_2$ for 24 h. The sensitivity to $CdCl_2$ was measured by colorimetric assay using alamarBlue (BioSource International, Camarillo, CA) as described previously (Kojima et al., 2005). Oxidized alamarBlue (blue) can be converted to the reduced form (pink) by active cells. The amount of reduced alamarBlue is used to monitor cellular viability and metabolic activity.

Assay for CpG island methylation by HpaII and MspI digestion. Total genomic DNAs (5 μg) were extracted from 5-aza-dC-treated and untreated A7 cells and untreated P cells by using a Wizard Genomic DNA Purification Kit (Promega) and digested with 100 U of either *Hpa*II or *Msp*I (New England Biolabs, Ipswich, MA) at 37 °C overnight. *Hpa*II is a methylation-sensitive restriction endonuclease that cleaves DNA at a CCGG sequence when the internal cytosine residue is unmethylated on both strands. *Msp*I cleaves DNA at a CCGG sequence regardless of methylation status and serves as a control for digestion efficiency. Digested DNA was then amplified by PCR using the primers covering the nucleotide from −89 to +894. PCR was performed in a solution as described above. The amplification profile was an initial denaturation at 94 °C for 3 min, then denaturation at 94 °C for 1 min, annealing at 55 °C for 1 min, and extension at 72 °C for 1 min. The reaction was repeated for 25–30 cycles. The following oligonucleotides were used for PCR primers of 5′ sense and 3′ antisense: 5′-GGGTTGCACAGTCAGAGGAT-3′ and 5′-CCGCCCTCAACTTCGTA-3′. PCR amplification products were analyzed by electrophoresis on a 1.5% agarose gel.

Methylation-specific PCR (MSP). Total genomic DNAs were extracted from A7 and P cells by using a Wizard Genomic DNA Purification Kit (Promega). Bisulfite modification of DNA (1 mg) was carried out with the CpGenome DNA Modification Kit (Intergen, Purchase, NY) according to the manufacturer's instructions. Modified DNA samples were precipitated with ethanol and resuspended in a TE buffer (10 mM Tris–HCl (pH 7.5) and 1 mM EDTA). The amplification profile for PCR was an initial denaturation at 94 °C for 3 min, then denaturation at 94 °C for 1 min, annealing at 55 °C for 1 min, and extension at 72 °C for 1 min. The reaction was repeated for 25–30 cycles. The primer sequences for MSP were designed with Methyl Primer Express Software v1.0 (Applied Biosystems, Foster City, CA). The primers for the unmethylated DNA in ZIP8 CpG were as follows: M1, 5′-GTTTTGATTTTTTATGTTTTTGT-3′ and 5′-TAACTCTCACTTATCCCAAATA-3′; M2, 5′-TTGAGATTGTAGAG-

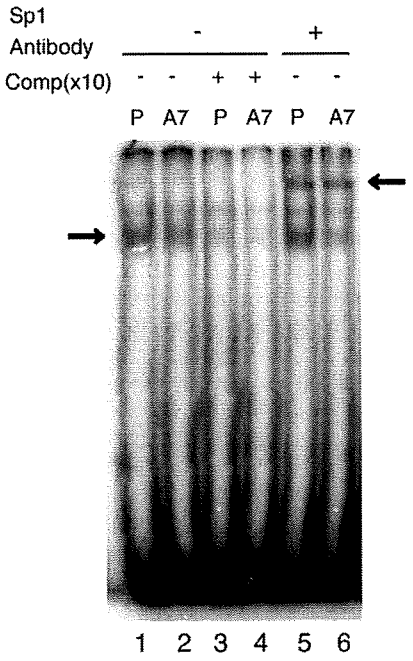

Fig. 1. Binding of Sp1 to the promoter of *slc39a8* was not different between cadmium-resistant (A7) and parental (P) cells. EMSA was carried out with nuclear protein extracts from A7 and P cells. DNA binding of Sp1 in the nuclear fraction was analyzed with a ^{32}P-labeled oligonucleotide probe for the Sp1 element. The specificity of Sp1-binding was determined by the addition of a 10-fold molar excess of unlabeled competitor oligonucleotides (lanes 3 and 4) and anti-Sp1 antibody for supershift (lanes 5 and 6). The left arrow indicates protein-DNA complexes, and the right arrow indicates the supershift bands.

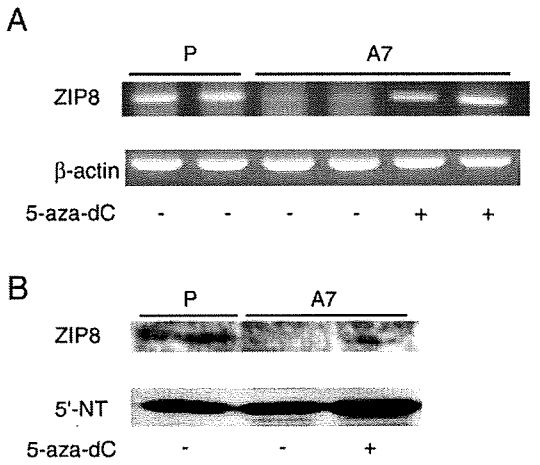

Fig. 2. Treatment of cadmium-resistant (A7) cells with 5-aza-dC resulted in the recovery of ZIP8 expression. (A) Total RNA was isolated from 5-aza-dC-treated and untreated A7 cells and untreated parental (P) cells. The mRNA levels of ZIP8 were determined by semiquantitative RT–PCR with ZIP8-specific primers. β-actin was used as a loading control. (B) The membrane fractions of A7 and P cells were subjected to Western blot analysis using an anti-ZIP8 antibody. 5′-NT was used as a loading control.

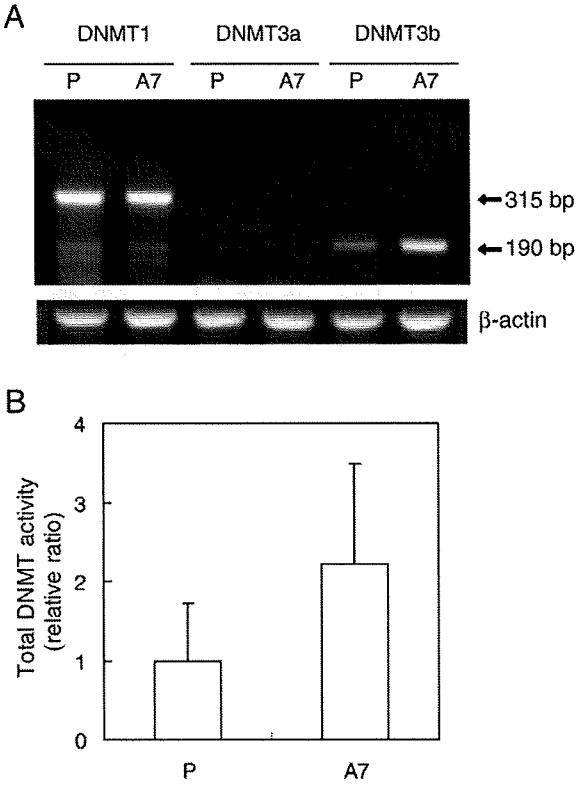

Fig. 3. The mRNA levels of DNMTs and total DNMT activity in cadmium-resistant (A7) and parental (P) cells. (A) Total RNAs were isolated from A7 and P cells and amplified by PCR with specific primers for DNMT1, DNMT3a, and DNMT3b. PCR products were analyzed on a 1.5% agarose gel. β-Actin was used as a loading control. (B) Total DNMT activity was determined with nuclear extracts from A7 and P cells. Data are presented as means ± SD ($n = 5$).

TGGGGGTAT-3′ and 5′-CCAAAATCTCAAACTCCAAACC-3′; and for methylated DNA in ZIP8 CpG: M1, 5′-TCGATTTTTTTACGTTTTTGC-3′ and 5′-ACTCTCGCTTATCCCGAAT-3′; M2, 5′-AGATTGTAGAGCGGGGGTAC-3′ and 5′-CCCGAAACCATCGTAAAAC-3′. PCR amplification products were analyzed by electrophoresis on a 1.5% agarose gel.

Statistics. Statistically significant differences were determined by Student's *t*-test.

Results

Binding of Sp1 to slc39a8 promoter

We first examined whether transactivation of the *slc39a8* gene by Sp1 is altered in A7 cells, since a recent study (Aiba et al., 2008) reported a decrease in DNA binding of Sp1 to the *slc39a8* promoter in the human lung cancer cell line SR3A in which ZIP8 expression was down-regulated by enhanced production of glutathione (GSH). As shown in Fig. 1, the binding of Sp1 in the nuclear extract of A7 cells to Sp1 consensus oligonucleotide probe was similar to that of P cells. The specificity of Sp1 binding to the probe was confirmed by the lack of binding in the presence of unlabeled probe and by the supershift analysis using antibody against Sp1 (Fig. 1). The intensities of the supershift bands were about the same between A7 and P cells. These data suggest that Sp1 binding to the *slc39a8* promoter was not significantly altered in A7 cells compared with P cells.

Recovery of the lowered ZIP8 expression by 5-aza-deoxycytidine treatment

To determine whether DNA methylation of the *slc39a8* gene is involved in the decreases in the mRNA and protein levels of ZIP8 in A7 cells, the effect of 5-aza-dC on the expression of ZIP8 was examined. The mRNA level of ZIP8 in A7 cells as determined by semiquantitative RT–PCR was markedly lower than that in P cells (Fig. 2A), confirming the result of real-time PCR assay in a previous study (Fujishiro et al., 2009). As shown in Fig. 2A, treatment of A7 cells with 5-aza-dC significantly increased the level of ZIP8 mRNA. In contrast, treatment of P cells with 5-aza-dC did not change the mRNA level of ZIP8 in P cells (data not shown). Western blot analysis showed that the protein level of ZIP8 in A7 cells was also very low, but treatment with 5-aza-dC recovered the protein level of ZIP8 in the membrane fraction of A7 cells (Fig. 2B). These data suggest that enhanced DNA methylation, which can be inhibited by 5-aza-dC, may be involved in the down-regulation of ZIP8 in A7 cells.

Expression and total activity of DNA methyltransferases in cadmium-resistant cells

As the involvement of DNA methylation in the down-regulation of ZIP8 in A7 cells was suggested, we next determined the expression and total activity of DNMTs in A7 and P cells. The mRNA levels of three DNMTs were determined by semiquantitative RT–PCR (Fig. 3A). There

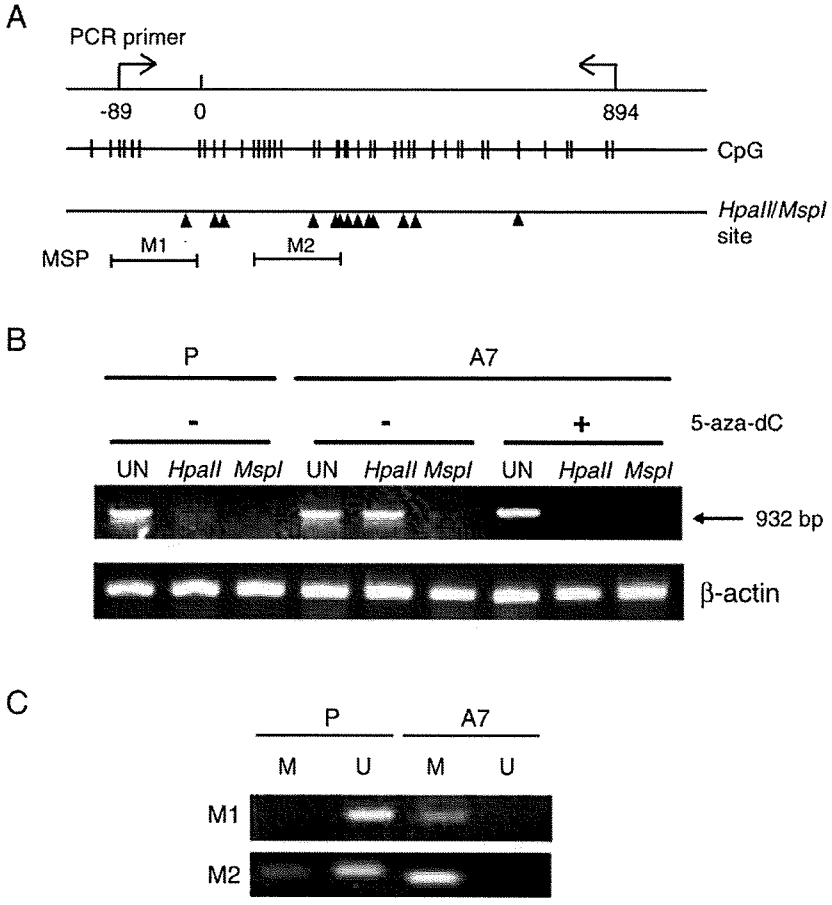

Fig. 4. The CpG island of the *slc39a8* gene is hypermethylated in cadmium-resistant (A7) cells. (A) Schematic representation of the putative CpG island of the *slc39a8* gene. A dense clustering of CpG dinucleotides, as indicated by vertical lines, indicates the CpG island of the *slc39a8* gene. *Hpa*II/*Msp*I recognition sites within the CpG island are indicated by triangles. M1 and M2 indicate the regions covered by the primer sets of MSP assay. (B) Genomic DNAs extracted from A7 and P cells were digested with *Hpa*II or *Msp*I and then amplified by PCR using the primers shown by the arrows in (A). The PCR bands in the lane of *Hpa*II digestion indicate the methylation of *Hpa*II recognition sites. Treatment of A7 cells with 5-aza-dC resulted in demethylation of CpG as indicated by the lack of a PCR band in the lane of *Hpa*II digestion. UN, uncut DNA. β-Actin was used as a loading control. (C) MSP analysis of *slc39a8* gene was performed using sodium bisulfite-modified DNA extracted from A7 and P cells. M and U indicate the reaction using the primers specific for methylated and unmethylated CpG sites, respectively. The primers were designed to cover M1 and M2 regions as indicated in the bottom of (A). The experiments were repeated three times.

was no difference in the mRNA levels of DNMT1 between A7 and P cells, and the signals of DMNT3a were not detected in either cell line. On the other hand, A7 cells showed a higher level of DMNT3b mRNA than P cells. To examine whether the increase in mRNA levels of DNMT3b actually contributed to enhanced DNA methylation of ZIP8, we determined total DNMT activity. As shown in Fig. 3B, total DNMT activity of A7 cells showed a higher tendency than that of P cells, although the difference was not statistically significant ($p = 0.096$).

Methylation of the CpG island of the slc39a8 gene

To determine whether the *slc39a8* gene is actually hypermethylated in cadmium-resistant cells, we examined the methylation status of the CpG island of the *slc39a8* gene in A7 and P cells by using methylation-sensitive and -insensitive digestion followed by a PCR. The CpG island of the *slc39a8* gene was predicted by a CpG island searcher [http://cpgislands.usc.edu/], and the region from −72 to +842 was found to harbor 13 *HpaII*/*MspI* sites (Fig. 4A). Genomic DNAs obtained from A7 and P cells were treated with *HpaII*, a methylation-sensitive restriction endonuclease, or with *MspI*, a methylation-insensitive restriction endonuclease, followed by PCR amplification with primers covering the nucleotide from −89 to +894 (Fig. 4A). The lack of amplified products in either *HpaII*- or *MspI*-digested DNA from P cells indicates that the CpG island of the *slc39a8* gene is not methylated under physiological conditions (Fig. 4B). On the other hand, a clear band of PCR amplification was found in *HpaII*-digested, but not in *MspI*-digested DNA from A7 cells, suggesting that the CpG island of the *slc39a8* gene in A7 cells is hypermethylated. In MSP assay (Fig. 4C), PCR products were detected by unmethylation-specific primers in P cells, while methylation-specific primers produced PCR products in A7 cells, confirming the CpG hypermethylation of *slc39a8* gene in A7 cells. Furthermore, treatment of A7 cells with 5-aza-dC resulted in the loss of the PCR product in *HpaII*-digested DNA, suggesting that the recovery of ZIP8 expression in A7 cells treated with 5-aza-dC (Fig. 2) is actually attributable to demethylation of the *slc39a8* gene.

Recovery of accumulation of and sensitivity to cadmium in A7 cells by treatment with 5-aza-deoxycytidine

To test whether enhanced methylation of the *slc39a8* gene actually contributes to the cadmium resistance in A7 cells, the effects of 5-aza-dC treatment on cadmium accumulation as well as cadmium cytotoxicity in A7 cells were examined. As shown in Fig. 4A, cadmium accumulation during 18 h after the addition of 1 μM $CdCl_2$ in A7 cells increased significantly by pretreatment with 5-aza-dC, although not to the same level as that of P cells. Reflecting the recovery of cadmium accumulation, the sensitivity of A7 cells to cadmium cytotoxicity was also enhanced by pretreatment with 5-aza-dC (Fig. 4B). The IC_{50} values of $CdCl_2$ in A7 cells were lowered from 53 μM to 26 μM (2-fold change) by 5-aza-dC treatment, although they were still higher than the IC_{50} values of $CdCl_2$ in P cells (10 μM). These data suggest that hypermethylation of genes including *slc39a8* in A7 cells actually contributes to the reduced accumulation of cadmium and the acquisition of cadmium resistance.

Discussion

Previously, we have developed MT-null cadmium-resistant (A7) cells which showed a marked decrease in cadmium uptake (Yanagiya et al., 1999, 2000). The characterization of these cells revealed that the expression of ZIP8, a zinc transporter encoded by *slc39a8*, was significantly suppressed (Fujishiro et al., 2009). Thus, the loss-of-function, but not the gain-of-function, of a particular transport system caused a decrease in cadmium influx in A7 cells. However, the mechanism underlying the lowered expression of ZIP8/*slc39a8* in A7 cells remains to be elucidated. In general, suppression of gene expression can be conferred by 1) a mutation in the gene including the promoter region, 2) a defect in the transcriptional machineries, or 3) an epigenetic silencing of the gene by DNA methylation. Because several lines of evidence have suggested that DNA methylation is enhanced by long-term exposure to cadmium (Takiguchi et al., 2003; Jiang et al., 2008; Benbrahim-Tallaa et al., 2007), we focused on DNA methylation as a potential cause of the down-regulation of *slc39a8* gene expression.

Treatment of A7 cells with 5-aza-dC resulted in an increase in the ZIP8 mRNA level and, consequently, an increase in the ZIP8 protein level (Fig. 2), suggesting a role of DNA hypermethylation in the suppression of *slc39a8* gene expression. Reflecting the recovery of ZIP8 protein expression, treatment of A7 cells with 5-aza-dC resulted in increases in cadmium accumulation and sensitivity (Fig. 5). These data suggest that the ability of the *slc39a8* gene to produce the mRNA and protein of ZIP8 was not completely disrupted in A7 cells, but only the transcription efficiency of the *slc39a8* gene was lowered. The inhibition of DNMTs by 5-aza-dC led to a recovery of the functional *slc39a8* gene and ZIP8 protein.

As shown in Fig. 3, the mRNA level of DNMT3b in A7 cells was higher than that in P cells, and a tendency of an increase in DNMT activity in A7 cells was found. In accordance with our data, three independent studies have shown that long-term exposure of cells to cadmium resulted in

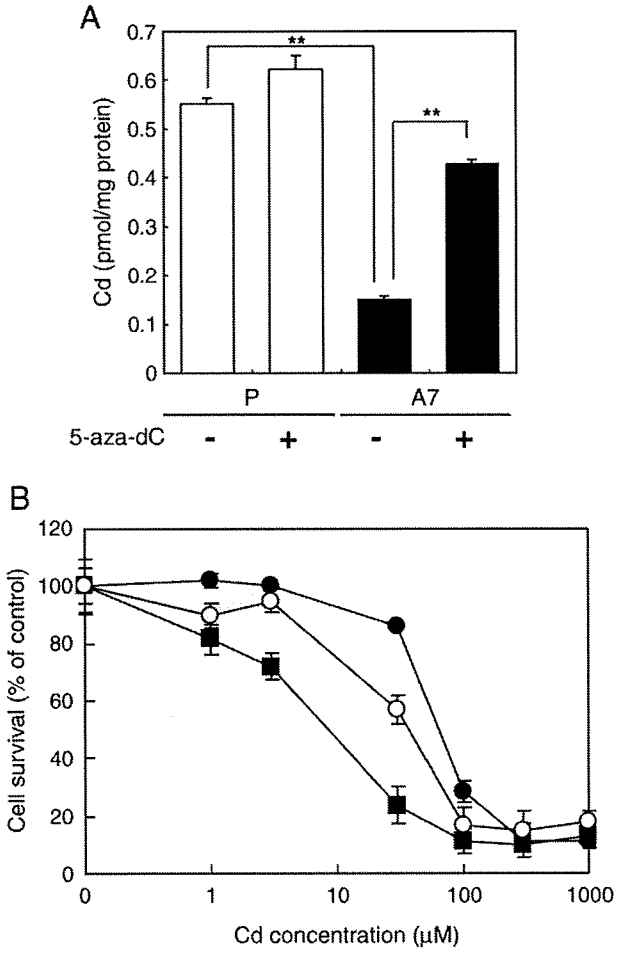

Fig. 5. Treatment of cadmium-resistant (A7) cells with 5-aza-dC resulted in the recovery of cadmium accumulation and sensitivity to cadmium. (A) A7 and P cells were treated with 5-aza-dC for 72 h and then exposed to $CdCl_2$ (1 μM) for 18 h. Cadmium accumulation was determined by using ^{109}Cd as a tracer. Data are presented as means ± SD. The experiments were repeated three times. **Significantly different from P cells or from untreated cells, $p<0.01$. (B) The sensitivity of A7 cells and P cells to $CdCl_2$ was examined by colorimetric assay with alamarBlue. 5-Aza-dC-treated (open circles) and untreated (closed circles) A7 cells and untreated P cells (closed squares) were exposed to $CdCl_2$ for 24 h. The data are presented as means ± SD ($n = 5$).

the activation of DNMTs (Takiguchi et al., 2003; Benbrahim-Tallaa et al., 2007; Jiang et al., 2008). Exposure of human embryo lung fibroblast cells to cadmium resulted in an increase in mRNA levels of DNMT1, DNMT3a, and DNMT3b (Jiang et al., 2008), while exposure of human prostate epithelial cells to cadmium for 10 weeks resulted in an increase in mRNA levels of DNMT3b but not of DNMT1 or DNMT3a (Benbrahim-Tallaa et al., 2007). Although it was originally recognized that DNMT1 is for the maintenance of DNA methylation and DNMT3a and DNMT3b are for de novo DNA methylation, recent studies have shown that a high expression of DNMT3b alone is detected in various cancer cells (Girault et al. 2003, Robertson et al. 1999, Saito et al. 2002, Lin et al., 2005), suggesting that DNMT3b plays important roles in both the development and maintenance of aberrant DNA methylation. However, further studies are necessary to clarify whether enhanced expression of DNMT3b alone is responsible for hypermethylation of *slc39a8* gene observed in this study.

We examined whether enhanced DNA methylation actually occurred in the *slc39a8* gene in A7 cells and found that the putative CpG island of the *slc39a8* gene in A7 cells was hypermethylated, but that of parental cells was not, by using both *Hpa*II/*Msp*I digestion assay (Fig. 4B) and MSP assay (Fig. 4C). Furthermore, treatment of A7 cells with 5-aza-dC resulted in the loss of methylcytosine in the CpG island of the *slc39a8* gene (Fig. 4B), suggesting that the effect of 5-aza-dC on the recovery of ZIP8 expression (Fig. 2) was actually due to the demethylation of the CpG island in the *slc39a8* gene. These data clearly indicate that DNA hypermethylation of the *slc39a8* gene is at least partly responsible for the down-regulation of ZIP8. As the CpG island of the *slc39a8* gene encompasses the region from −72 to +842 (Fig. 4A), which covers the 5′-flanking region, exon 1, and intron 1, it is possible that the methylation status in exon 1 or intron 1 rather than the methylation status in the promoter region is responsible for epigenetic regulation of *slc39a8* gene expression. In support of this notion, many studies have shown that hypermethylation in the initial exon or intron plays an important role in epigenetic regulation of a variety of genes, such as *IGFBP7* (Lin et al., 2007), *GPx3* (Yu et al., 2007), *HSulf-1* (Staub et al., 2007), *CYP2W1* (Karlgren et al., 2006), *TCF4* (Kim et al., 2008), and *TCF21* (Shivapukar et al., 2008).

The transcriptional regulation mechanisms of the *slc39a8* gene have been poorly elucidated. Recently, Aiba et al. (2008) reported that the increase in cellular GSH caused by over-expression of the GCLC subunit in the human lung cancer cells led to the down-regulation of ZIP8 via the reduction of Sp1 binding to the promoter of *slc39a8*. These cells exhibited cadmium resistance due to the decreased accumulation of cadmium. However, no difference in Sp1 binding to the promoter of the *slc39a8* gene was found between A7 and P cells (Fig. 1), suggesting that Sp1 is not involved in down-regulation of the *slc39a8* gene in A7 cells. As cellular GSH levels in A7 cells were similar to those in P cells (data not shown), the regulation of *slc39a8* by Sp1 may be affected only by the change in cellular GSH levels.

Transcriptional and post-transcriptional regulation mechanisms of other ZIP family members such as ZIP4 and ZIP14 have been well investigated since ZIP4 responds to zinc deficiency and overload (Dufner-Beattie et al., 2003; Mao et al., 2007) and ZIP14 responds to an inflammatory cytokine, namely, interleukin-6 (Liuzzi et al., 2005). However, epigenetic regulation of ZIP family genes has not yet been reported. On the other hand, there is mounting evidence that DNA methylation is involved in the down-regulation of human solute carrier family transporters such as SLC5A8, a pancreatic sodium monocarboxylate cotransporter (Hong et al., 2005), SLC22A8, an organic anion transporter 3 (Kikuchi et al., 2006), SLC1A2, an astroglial glutamate transporter (Zschocke et al., 2007), SLC6A4, a serotonin reuptake transporter (Philibert et al., 2007), and SLC46A1, a proton-coupled folate transporter (Gonen et al., 2008).

In this decade, the relationship between carcinogenesis and epigenetic up-regulation of oncogenes or down-regulation of tumor-suppressor genes has been extensively explored (Gopalakrishnan et al., 2008). In particular, the carcinogenicity of nickel and arsenic compounds has been shown to be associated with aberrant DNA hypermethylation or hypomethylation (Zhao et al., 1997; Lee et al., 1998; Cui et al., 2006; Chanda et al., 2006; Salnikow and Zhitkovich, 2008). Cadmium-induced enhancement of DNMT activity has also been linked to the transformation of non-malignant cells (Takiguchi et al., 2003; Benbrahim-Tallaa et al., 2007). In addition, recent studies have shown that aberrant DNA methylation is responsible not only for oncogenesis but also for the acquisition of resistance against anti-tumor drugs (Chekhun et al., 2006, 2007; Reed et al., 2008). In the present study, we demonstrated that DNA hypermethylation of a metal transporter gene is involved in the acquisition of resistance against a toxic metal. Further studies are required to clarify the roles of epigenetic regulation of the genes involved in sensitivity to and protection against environmental toxicants as well as carcinogens.

Acknowledgments

We thank Dr. H. Haba, RIKEN Wako Institute, for the assistance in producing radioactive ^{109}Cd. This work was partly supported by a Grant-in-Aid for Scientific Research (B-19390169) from the Japan Society for the Promotion of Science and by a Grant-in-Aid for Young Scientists (B-10389182) from the Ministry from Education, Culture, Sport, Science, and Technology, Japan.

References

Aiba, I., Hossain, A., Kuo, M.T., 2008. Elevated GSH increases cadmium resistance through down-regulation of Sp1-dependent expression of the cadmium transporter ZIP8. Mol. Pharmacol. 74, 823–833.

Benbrahim-Tallaa, L., Waterland, R.A., Dill, A.L., Webber, M.M., Waalkes, M.P., 2007. Tumor suppressor gene inactivation during cadmium-induced malignant transformation of human prostate cells correlates with overexpression of de novo DNA methyltransferase. Environ. Health Perspect. 115, 1454–1459.

Chanda, S., Dasgupta, U.B., Guhamazumder, D., Gupta, M., Chaudhuri, U., Lahiri, S., Das, S., Ghosh, N., Chatterjee, D., 2006. DNA hypermethylation of promoter of gene p53 and p16 in arsenic-exposed people with and without malignancy. Toxicol. Sci. 89, 431–437.

Chekhun, V.F., Kulik, G.I., Yurchenko, O.V., Tryndyak, V.P., Todor, I.N., Luniv, L.S., Tregubova, N.A., Pryzimirska, T.V., Montgomery, B., Rusetskaya, N.V., Pogribny, I.P., 2006. Role of DNA hypomethylation in the development of the resistance to doxorubicin in human MCF-7 breast adenocarcinoma cells. Cancer Lett. 231, 87–93.

Chekhun, V.F., Lukyanova, N.Y., Kovalchuk, O., Tryndyak, V.P., Pogribny, I.P., 2007. Epigenetic profiling of multidrug-resistant human MCF-7 breast adenocarcinoma cells reveals novel hyper- and hypomethylated targets. Mol. Cancer Ther. 6, 1089–1098.

Cui, X., Wakai, T., Shirai, Y., Hatakeyama, K., Hirano, S., 2006. Chronic oral exposure to inorganic arsenate interferes with methylation status of p16^{INK4a} and RASSF1A and induces lung cancer in A/J mice. Toxicol. Sci. 91, 372–381.

Dalton, T.P., He, L., Wang, B., Miller, M.L., Jin, L., Stringer, K.F., Chang, X., Baxter, C.S., Nebert, D.W., 2005. Identification of mouse *slc39a8* as the transporter responsible for cadmium-induced toxicity in the testis. Proc. Natl. Acad. Sci. U. S. A. 102, 3401–3406.

Donai, H., Morinaga, H., Yamauchi, T., 2001. Genomic organization of neuronal cell type specific promoter activity of b isoform of Ca^{2+}/calmodulin dependent protein kinase II of rat brain. Mol. Brain. Res. 94, 35–47.

Dufner-Beattie, J., Langmade, S.J., Wang, F., Eide, D., Andrews, G.K., 2003. Structure, function, and regulation of a subfamily of mouse zinc transporter genes. J. Biol. Chem. 278, 50142–50150.

Fujishiro, H., Okugaki, S., Nagao, S., Satoh, M., Himeno, S., 2006. Characterization of gene expression profiles of metallothionein-null cadmium-resistant cells. J. Health. Sci. 52, 292–299. http://www.jstage.jst.go.jp/article/jhs/52/3/52_292/_article. doi:10.1248/jhs.52.292.

Fujishiro, H., Okugaki, S., Kubota, K., Fujiyama, T., Miyataka, H., Himeno, S., 2009. The role of ZIP8 down-regulation in cadmium-resistant metallothionein-null cells. J. Appl. Toxicol. 29, 367–373.

Girault, I., Tozlu, S., Lidereau, R., Bièche, I., 2003. Expression analysis of DNA methyltransferases 1, 3A, and 3B in sporadic breast carcinomas. Clin. Cancer Res. 9, 4415–4422.

Gonen, N., Bram, E.E., Assaraf, Y.G., 2008. PCFT/SLC46A1 promoter methylation and restoration of gene expression in human leukemia cells. Biochem. Biophys. Res. Commun. 376, 787–792.

Gopalakrishnan, S., Van Emburgh, B.O., Robertson, K.D., 2008. DNA methylation in development and human disease. Mutat. Res. 647, 30–38.

Gunshin, H., Mackenzie, B., Berger, U.V., Gunshin, Y., Romero, M.F., Boron, W.F., Nussberger, S., Gollan, J.L., Hediger, M.A., 1997. Cloning and characterization of a mammalian proton-coupled metal-ion transporter. Nature 388, 482–488.

Haba, H., Enomoto, S., 2005. Radioactive tracers produced at RIKEN accelerator research facility and future RI beam factory. RIKEN Accel. Prog. Rep. 38, 105–106.

He, L., Girijashanker, K., Dalton, T.P., Reed, J., Li, H., Soleimani, M., Nebert, D.W., 2006. ZIP8, member of the solute-carrier-39 (SLC39) metal-transporter family: characterization of transporter properties. Mol. Pharmacol. 70, 171–180.

Himeno, S., 2002. Application of metallothionein null cells to investigation of cadmium transport. J. Inorg. Biochem. 88, 207–212.

Himeno, S., Yanagiya, T., Fujishiro, H., 2009. The role of zinc transporters in cadmium and manganese transport in mammalian cells. Biochimie 91, 1218–1222.

Hong, C., Maunakea, A., Jun, P., Bollen, A.W., Hodgson, J.G., Goldenberg, D.D., Weiss, W.A., Costello, J.F., 2005. Shared epigenetic mechanisms in human and mouse gliomas inactivate expression of the growth suppressor SLC5A8. Cancer Res. 65, 3617–3623.

Jiang, G., Xu, L., Song, S., Zhu, C., Wu, Q., Zhang, L., Wu, L., 2008. Effects of long-term low-dose cadmium exposure on genomic DNA methylation in human embryo lung fibroblast cells. Toxicology 244, 49–55.

Karlgren, M., Gomez, A., Stark, K., Svärd, J., Rodriguez-Antona, C., Oliw, E., Bernal, M.L., Cajal, S.R. y., Johansson, I., Ingelman-Sundberg, M., 2006. Tumor-specific expression of the novel cytochrome P450 enzyme, CYP2W1. Biochem. Biophys. Res. Commun. 341, 451–458.

Kikuchi, R., Kusuhara, H., Hattori, N., Shiota, K., Kim, I., Gonzalez, F.J., Sugiyama, Y., 2006. Regulation of the expression of human organic anion transporter 3 by hepatocyte nuclear factor 1 α/β and DNA methylation. Mol. Pharmacol. 70, 887–896.

Kim, S-K., Jang, H-R., Kim, J-H., Kim, M., Noh, S-M., Song, K-S., Kang, G.H., Kim, H.J., Kim, S-Y., Yoo, H-S., Kim, Y.S., 2008. CpG methylation in exon 1 of *transcription factor 4* increases with age in normal gastric mucosa and is associated with gene silencing in intestinal-type gastric cancers. Carcinogenesis 29, 1623–1631.

Kojima, C., Sakurai, T., Waalkes, M.P., Himeno, S., 2005. Cytolethality of glutathione conjugates with monomethylarsenic or dimethylarsenic compounds. Biol. Pharm. Bull. 28, 1827–1832.

Kraus, K.A., Nelson, F., 1955. 1st International Conference on the Peaceful Uses of Atomic Energy, Paper 837.

Lee, Y.W., Broday, L., Costa, M., 1998. Effects of nickel on DNA methyltransferase activity and genomic DNA methylation levels. Mutat. Res. 415, 213–218.

Lin, T-S., Lee, H., Chen, R-A., Ho, M-L., Lin, C-Y., Chen, Y-H., Tsai, Y.Y., Chou, M-C., Cheng, Y-W., 2005. An association of DNMT3b protein expression with $P16^{INK4a}$ promoter hypermethylation in non-smoking female lung cancer with human papillomavirus infection. Cancer Lett. 226, 77–84.

Lin, J., Lai, M., Huang, Q., Ma, Y., Cui, J., Ruan, W., 2007. Methylation patterns of *IGFBP7* in colon cancer cell lines are associated with levels of gene expression. J. Pathol. 212, 83–90.

Liu, Z., Li, H., Soleimani, M., Girijashanker, K., Reed, J.M., He, L., Dalton, T.P., Nebert, D.W., 2007. Cd^{2+} versus Zn^{2+} uptake by the ZIP8 HCO_3^--dependent symporter: kinetics, electrogenicity and trafficking. Biochem. Biophys. Res. Commun. 365, 814–820.

Liuzzi, J.P., Lichten, L.A., Rivera, S., Blanchrd, R.K., Aydemir, T.B., Knutson, M.D., Ganz, T., Cousins, R.J., 2005. Interleukin-6 regulates the zinc transporter Zip14 in liver and contributes to hypozincemia of the acute-phase response. Proc. Natl. Acad. Sci. U. S. A. 102, 6843–6848.

Mao, X., Kim, B-E., Wang, F., Eide, D.J., Petris, M.J., 2007. A histidine-rich cluster mediate the ubiquitination and degradation of the human zinc transporter, hZIP4, and protects against zinc cytotoxicity. J. Biol. Chem. 282, 6992–7000.

Min, K-S., Ueda, H., Tanaka, K., 2008. Involvement of intestinal calcium transporter 1 and metallothionein in cadmium accumulation in the liver and kidney of mice fed a low-calcium diet. Toxicol. Lett. 176, 85–92.

Philibert, R., Madan, A., Andersen, A., Cadoret, R., Packer, H., Sandhu, H., 2007. Serotonin transporter mRNA levels are associated with the methylation of an upstream CpG island. Am. J. Genet. B. Neuropsychiatr. Genet. 144B, 101–105.

Reed, K., Hembruff, S.L., Laberge, M.L., Villeneuve, D.J., Côté, G.B., Parissenti, A.M., 2008. Hypermethylation of the ABCB1 downstream gene promoter accompanies *ABCB1* gene amplification and increased expression in docetaxel-resistant MCF-7 breast tumor cells. Epigenetics 3, 270–280.

Robertson, K.D., Uzvolgyi, E., Liang, G., Talmadge, C., Sumegi, J., Gonzales, F.A., Jones, P.A., 1999. The human DNA methyltransferases (DNMTs) 1, 3a and 3b: coordinate mRNA expression in normal tissues and overexpression in tumors. Nucleic Acids Res. 27, 2291–2298.

Saito, Y., Kanai, Y., Sakamoto, M., Saito, H., Ishii, H., Hirohashi, S., 2002. Overexpression of a splice variant of DNA methyltransferase 3b, DNMT3b4, associated with DNA hypomethylation on pericentromeric satellite regions during human hepatocarcinogenesis. Proc. Natl. Acad. Sci. U. S. A. 99, 10060–10065.

Salnikow, K., Zhitkovich, A., 2008. Genetic and epigenetic mechanisms in metal carcinogenesis and cocarcinogenesis: nickel, arsenic, and chromium. Chem. Res. Toxicol. 21, 28–44.

Shivapukar, N., Stastny, V., Xie, Y., Prinsen, C., Frenkel, E., Czerniak, B., Thunnissen, F.B., Minna, J.D., Gazdar, A.F., 2008. Differential methylation of a short CpG-rich sequence within exon 1 of *TCF21* gene: a promising cancer biomarker assay. Cancer Epidemiol. Biomarkers. Prev. 17, 995–1000.

Staub, J., Chien, J., Pan, Y., Qian, X., Narita, K., Aletti, G., Scheerer, M., Roberts, L.R., Molina, J., Shridhar, V., 2007. Epigenetic silencing of HSulf-1 in ovarian cancer: implications in chemoresistance. Oncogene 26, 4969–4978.

Takiguchi, M., Achanzar, W.E., Qu, W., Li, G., Waalkes, M.P., 2003. Effects of cadmium on DNA-(cytosine-5) methyltransferase activity and DNA methylation status during cadmium-induced cellular transformation. Exp. Cell. Res. 286, 355–365.

Valberg, L.S., Sorbie, J., Hamilton, D.L., 1976. Gastrointestinal metabolism of cadmium in experimental iron deficiency. Am. J. Physiol. 231, 462–467.

Wang, B., Schneider, S.N., Dragin, N., Girijashanker, K., Dalton, T.P., He, L., Miller, M.L., Stringer, K.F., Soleimani, M., Richardson, D.D., Nebert, D.W., 2007. Enhanced cadmium-induced testicular necrosis and renal proximal tubule damage caused by gene-dose increase in a Slc39a8-transgenic mouse line. Am. J. Physiol. Cell. Physiol. 292, C1523–C1535.

Washko, P.W., Cousins, R.J., 1977. Role of dietary calcium and calcium binding protein in cadmium toxicity in rats. J. Nutr. 107, 920–928.

Yanagiya, T., Imura, N., Kondo, Y., Himeno, S., 1999. Reduced uptake and enhanced release of cadmium in cadmium-resistant metallothionein null fibroblasts. Life Sci. 65, 177–182.

Yanagiya, T., Imura, N., Kondo, Y., Himeno, S., 2000. Suppression of a high-affinity transport system for manganese in cadmium-resistant metallothionein null cells. J. Pharmacol. Exp. Ther. 292, 1080–1086.

Yu, Y.P., Yu, G., Tseng, G., Cieply, K., Nelson, J., Defrances, M., Zarnegar, R., Michalopoulos, G., Luo, J-H., 2007. Glutathione peroxidase 3, deleted or methylated in prostate cancer, suppresses prostate cancer growth and metastasis. Cancer Res. 67, 8043–8050.

Zhao, C.Q., Young, M.R., Diwan, B.A., Coogan, T.P., Waalkes, M.P., 1997. Association of arsenic-induced malignant transformation with DNA hypomethylation and aberrant gene expression. Proc. Natl. Acad. Sci. U. S. A. 94, 10907–10912.

Zschocke, J., Allritz, C., Engele, J., Rein, T., 2007. DNA methylation dependent silencing of the human glutamate transporter *EAAT2* gene in glial cells. Glia 55, 663–674.

J. Radiat. Res., 50, 407–413 (2009)

An Approach to Estimate Radioadaptation from DSB Repair Efficiency#

Fumio YATAGAI[1]*, Kaoru SUGASAWA[2], Shuichi ENOMOTO[1] and Masamitsu HONMA[3]

Radioadaptation/I-SceI digestion/DSB repair/TK6 cells.

In this review, we would like to introduce a unique approach for the estimation of radioadaptation. Recently, we proposed a new methodology for evaluating the repair efficiency of DNA double-strand breaks (DSB) using a model system. The model system can trace the fate of a single DSB, which is introduced within intron 4 of the *TK* gene on chromosome 17 in human lymphoblastoid TK6 cells by the expression of restriction enzyme I-SceI. This methodology was first applied to examine whether repair of the DSB (at the I-SceI site) can be influenced by low-dose, low-dose rate gamma-ray irradiation. We found that such low-dose IR exposure could enhance the activity of DSB repair through homologous recombination (HR). HR activity was also enhanced due to the pre-IR irradiation under the established conditions for radioadaptation (50 mGy X-ray–6 h–I-SceI treatment). Therefore, radioadaptation might account for the reduced frequency of homozygous loss of heterozygosity (LOH) events observed in our previous experiment (50 mGy X-ray–6 h–2 Gy X-ray). We suggest that the present evaluation of DSB repair using this I-SceI system, may contribute to our overall understanding of radioadaptation.

INTRODUCTION

It is important to accurately estimate human health risks for persons occupationally exposed to ionizing radiation (IR), such as airline crews and workers in medical and industrial fields. For estimating such risks, it is worthwhile to investigate radioadaptation, that is, acquiring a cellular radioresistance to a challenging IR by a pre-exposure to low-dose IR. Radioadaptation was first reported by Olivieri *et al.*[1] The priming radiation exposure delivered by labeling human lymphocytes with tritiated thymidine caused a decrease in chromosomal aberration frequency after a challenging exposure to 1.5 Gy of IR. That discovery stimulated a series of studies using human lymphocytes and various mammalian cell lines as described in reviews.[2,3] A reduced induction of both micronuclei and sister chromatid exchanges was shown in Chinese hamster V79 cells pre-exposed to low doses of γ-rays or ^{3}H β-rays.[4] Subsequent studies reported similar radioadaptive responses, such as reduced mutation frequencies in human lymphocytes,[5] mouse SR-1 cells[6] and human-hamster hybrid A_L cells,[7] an altered mutation spectrum in human-hamster hybrid A_L cells,[7] reduced micronucleus frequencies in human lymphocytes[8] and mouse embryo cells,[9] and reduced deletions and rearrangements in human lymphoblast cells.[10] Those studies suggest that radioadaptation is an important defense mechanism against a high-dose IR, although the molecular mechanisms involved remain largely unknown.[11–15]

Cellular responses such as a bystander effect, genetic instability, and hyper-radiosensitivity are reported to be tightly related to the radioadaptation.[16–21] In mammalian cells, for example, bystander mutagenesis may be suppressed by an adaptive response.[16] Another example is the possible involvement of a "radioadaptive bystander" effect in human lung fibroblasts.[22] The reduction of radiosensitivity in cells with a wild type *p53* gene by a radiation-induced, nitric oxide (NO)-mediated bystander effect may also be a manifestation of the radioadaptation.[21,23] This possibility is supported by the finding that the NO-induced apoptosis observed in lymphoblastoid and fibroblast cells depends on the phosphorylation and activation of p53.[24] In fact, p53 was suggested to play a key role in the mechanisms of an adaptive response

*Corresponding author: Phone: +81-48-467-9710,
Fax: +81-48-467-9710,
E-mail: yatagai@riken.jp

[1]Metallomics Imaging Research Unit, Center for Molecular Imaging Science, The Institute of Physical and Chemical Research (RIKEN), Saitama 351-0198, Japan; [2]Biosignal Research Center, Kobe University, Hyogo 657-8501, Japan; [3]Division of Genetics and Mutagenesis, National Institute of Health Sciences, Tokyo 158-8501, Japan.

#Translated and modified from Radiat. Biol. Res. Comm. Vol.43(4); 443–453, (2008, in Japanese).
doi:10.1269/jrr.09050

mediated by a feedback signaling pathway involving protein kinase C (PKC), p38 mitogen activated protein kinase (p38MAPK), and phospholipase C (PLC).[11,13,25]

One of the possible targets for radioadaptation is oxidative base damage. A low-dose rate whole body γ-irradiation of mice (1.2 mGy/h, total 0.5 Gy) demonstrated the activation of antioxidative enzymes such as MnSOD and catalase in spleen cells, leading to less DNA damage as determined by a comet assay.[26] Furthermore, down-regulation of the human *CDC16* gene that occurs after oxidative stress causes more rapid and efficient repair in adapted (2 cGy pre-irradiated) human lymphoblastoid cells challenged with 4 Gy irradiation.[12] However, oxidative base excision repair enzymes, including DNA glycosylases, hOGG1, and hNth1, are reportedly not up-regulated at the post-transcriptional level in γ-ray-primed TK6 cells.[27] Those reports suggest that the antioxidant defense machinery is likely to be involved in radioadaptation although the mechanisms involved are still not well understood.

Gene expression also seems to be tightly related to a variety of functions in the adaptive response such as the induction of antioxidant defense machinery, repair of DNA damage, control of cell-cycle progression, *etc.* In fact, *de novo* synthesis of transcripts and proteins is reported to be required for the expression of the adaptive response.[28] Following that report, gene expression analysis has been extensively studied by many investigators.[15,28–31] For example, the *CHD6* gene in human lymphoblastoid cell AHH-1 can be up-regulated by 0.5 Gy of γ-irradiation and its induced expression could be involved in a low-dose hypersensitive response.[29] Recently, gene profiles in the kidney and testis from γ-irradiated (485 days at dose rates of 0.032–13 μGy/min) mice were determined using oligonucleotide microarrays, and differentially expressed genes were identified.[31]

DNA double strand breaks (DSBs) are a most serious type of DNA damage. They can be caused by IR or radiomimetic chemicals, and they can occur spontaneously during DNA replication. The nonrepair or misrepair of DSBs can cause cell death or mutagenic and/or carcinogenic consequences, so the accurate repair of DSBs is important for maintaining genomic integrity.[32,33] In other words, DSB repair is an essential function in all living organisms. Recently analyses using nondividing lymphocyte and fibroblast cells suggested that the adaptive response is not mediated by an enhanced rejoining of DNA strand breaks but rather is a reflection of perturbation in cell cycle progression.[34] On the other hand, the induction of an efficient chromosome repair system by the priming radiation dose is considered to be involved in radioadaptation mechanisms, and in fact, the efficiency of DSB repair in Chinese hamster V79 cells exposed to γ-rays is enhanced by a priming exposure of 5 cGy of γ-rays.[35] The reduced frequencies of chromosomal alterations as described above supports the latter possibility of DSB-repair enhancement. At the present stage, it is difficult to conclude which factor, cell-cycle perturbation or DSB repair, largely contributes to radioadaptation.

THE I-SCEI SYSTEM FOR DSB REPAIR EVALUATION

Outline of the system

A model system was constructed for evaluating DSB repair by tracing the fate of a single DSB on chromosomal DNA. The DSB generated in this system can be considered as a target DNA-lesion susceptible to repair, and this system can distinguish two major DSB repair pathways, non-homologous end-joining (NHEJ) and homologous recombination (HR) (Fig. 1).[36,37] The human lymphoblastoid cell line TSCE5 is heterozygous (+/–) for the thymidine kinase (*TK*) gene and the line TSCER2 is compound heterozygous (–/–; two different TK^- alleles); both carry an I-SceI endonuclease recognition site in intron 4 on one allele of the *TK* gene. DSBs can be generated at the I-SceI site by expression of the I-SceI vector.[36,37] When DSBs occur at the *TK* locus, NHEJ in TSCE5 cells produces TK-deficient mutants while HR between the *TK* alleles in TSCER2 cells produces TK-proficient revertants. This means that positive-negative drug selection for TK phenotypes permits distinction between NHEJ and HR repair.

Cell line construction for use in the system

Details of the strain construction are described in our previous work (Fig. 2).[36] Briefly, in lymphoblastoid TK6 cells heterozygous for the *TK* gene, the functional allele was first inactivated by gene targeting with vector pTK4 to

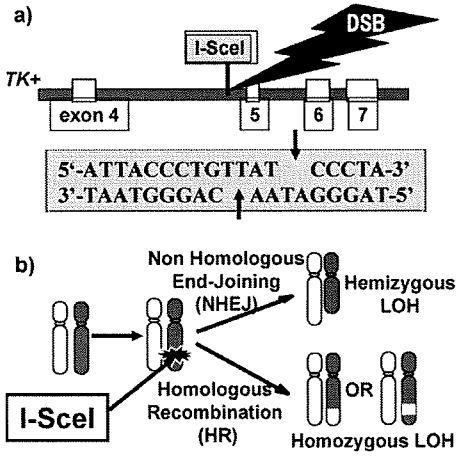

Fig. 1. Principle of DSB formation and repair evaluation. A single DNA double strand break (DSB) is generated at the I-SceI recognition site in a human lymphoblastoid TK6 cell by transfecting an I-SceI expression vector (a) and the efficiencies of DSB repair through non-homologous end-joining (NHEJ) or homologous repair (HR) are evaluated from induction of hemizygous and homozygous LOH events, respectively (see text).

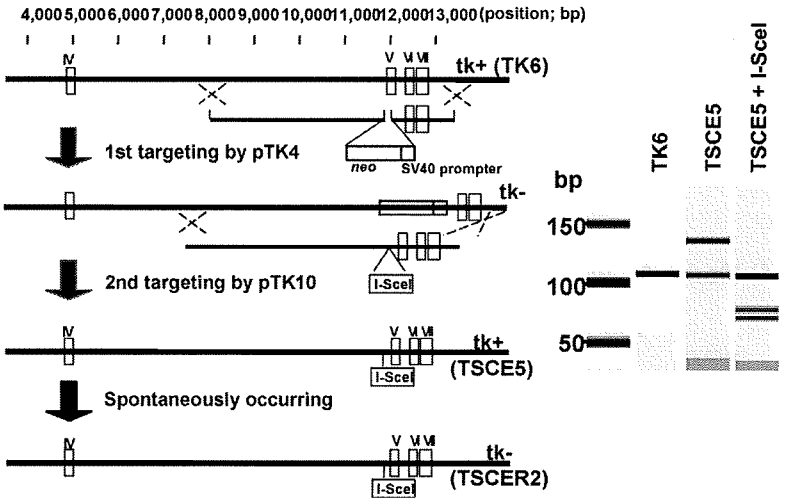

Fig. 2. Cell line construction. In the TK6 cell line, the functional allele of *TK* gene was first inactivated by gene targeting vector pTK4 and then the I-SceI recognition site was introduced at 75 bp upstream of exon 5 in the *TK* gene. The new line was termed TSCE5 and its compound heterozygote (*TK*–/–) cell line, TSCER2, was also isolated (see text).

replace exon 5 of the *TK* gene by a *neo* gene. To introduce the I-SceI recognition site at 75 bp upstream of exon 5, the targeting vector pTK10, encompassing about 6 kb of the original *TK* gene with exons 5, 6, and 7, and the I-SceI recognition site in intron 4, was used to revert the *TK* gene disrupted by pTK4. The new line was termed TSCE5. A spontaneous mutation in a TSCE5 cell (G to A in position 23 of exon 5), which we cloned, led to the compound heterozygote (*TK*–/–) cell line, TSCER2.

I-SceI expression for introduction of DSB

We introduced the I-SceI expression vector (pCBASce) by electroporation methodology using Nucleofector Kit V (amaxa AG, Cologne, Germany) (Fig. 3).[36–38] The I-SceI expression vector was introduced into about 65% of the cells at 24 hr after the transfection and the expression last for 3 days incubation.[37] The relatively long expression allowed us to succeed in estimating the influence of low-dose, low-dose-rate γ-rays irradiation on DSB repair, especially the effect of post-IR-exposure, as described below.

Evaluation of DSB repair efficiencies

Measurements of TK^- mutants and TK^+ revertants allow us to evaluate DSB repair efficiencies through NHEJ and HR pathways, respectively (Fig. 3). In TSCE5, when a DSB at the I-SceI site is repaired by NHEJ involving a deletion in the adjacent exon, the cell can be isolated as a TK-deficient mutant. In TSCER2, when a DSB is repaired by HR between the *TK* alleles, a TK^+ allele can be generated, resulting in a revertant phenotype. The DSB repair *via* NHEJ was 73–86 times higher than that *via* HR in our previous studies.[36,37] These findings are consistent with the report that NHEJ is the major repair pathway in mammalian cells.[39]

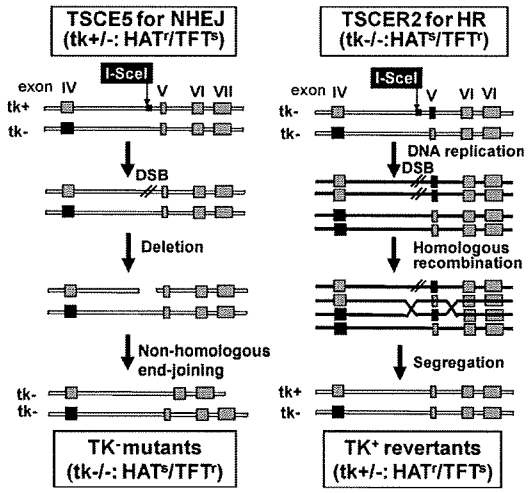

Fig. 3. An approach to evaluate DSB repair efficiency. In TSCE5, when a DSB at the I-SceI site is repaired by NHEJ involving a deletion in the adjacent exon, the cell can be isolated as a TK-deficient mutant. In TSCER2, when a DSB is repaired by HR between the *TK* alleles, a TK^+ allele can be generated, resulting in a revertant phenotype (see text). Filled exons represent TK mutations.

APPLICATION OF THE I-SCEI SYSTEM FOR EVALUATING RADIOADAPTATION IN TERMS OF DSB REPAIR

Influence of low-dose, low-dose-rate γ-rays on DSB repair

The I-SceI digestion system was applied for estimating the influence of low-dose, low-dose-rate γ-irradiation on repair of a site-specifically introduced DSB (Fig. 4).[38] The results